ChemComm

Dynamic Article Links

Cite this: *Chem. Commun.*, 2012, **48**, 3262–3278

www.rsc.org/chemcomm

FEATURE ARTICLE

Polymeric assemblies and nanoparticles with stimuli-responsive fluorescence emission characteristics

Changhua Li and Shiyong Liu*

Received 8th December 2011, Accepted 7th February 2012
DOI: 10.1039/c2cc17695e

Fluorescent polymeric assemblies and nanoparticles (NPs) of nanoscale dimensions have become a focus of intensive investigations during the past few decades due to combined advantages such as improved biocompatibility, water dispersibility, stimuli-responsiveness, facile integration into optical detection devices, and the ability of further functionalization. In addition, the chemical composition and morphology of polymeric assemblies and NPs can be modulated *via* synthetic approaches, leading to the precise spatial organization of multiple fluorophores. Thus, polymeric assemblies and NPs have been utilized to optimize the photoluminescent properties of covalently or physically attached fluorophores and facilely modulate the fluorescence resonance energy transfer (FRET) processes when the polymeric matrix is endowed with stimuli-responsiveness. These fascinating fluorescent polymeric assemblies and NPs offer unique and versatile platforms for the construction of novel detection, imaging, biolabeling, and optoelectronic systems. This feature article focuses on the recent developments of polymeric assemblies and NPs-based stimuli-tunable fluorescent systems and highlights their future practical applications with selected literature reports.

1. Introduction

The fluorescence technique has been widely used in diverse fields ranging from optical materials, analytical chemistry, protein conformation studies to biological assays by taking advantage of its exquisite sensitivity (even at the single molecule level) and selectivity, cost-effectiveness, facile operation, and superb spatial and temporal resolutions.[1–6] In addition, it enables the design of a new generation of fluorescent chemosensors and biosensors *via* the facile modulation of relevant photophysical properties of fluorophores when combined with proton-, energy- and electron-transfer processes, heavy-atom effects, changes of electronic density, and destabilization of a non-emissive $n\pi^*$ excited state.[6–8] Recently, fluorescence resonance energy transfer (FRET) has been utilized for designing chemosensors and biosensors to achieve quantitative ratiometric sensing, which can effectively eliminate background interferences and the fluctuation of detection conditions through the self-calibration of two emissive bands.[9] Moreover, it has also been introduced to the field of studying protein binding/interactions and exchanging dynamics of guest molecules encapsulated within polymeric assemblies and those occurred between unimer chains and polymeric micelles.[10–12] In addition, fluorescent lifetimes can offer extra information. One of the limitations of conventional small molecule-based fluorescent assays is the relatively poor solubility, especially in water, which considerably hinders their practical applications. Furthermore, most of these small molecule-based fluorescent assays lack the appropriate biocompatibility for real applications in biomedical investigations.

Recently, fluorescent polymeric assemblies and nanoparticles (NPs) have attracted ever-increasing attention owing to their superior advantages over conventional small molecule-based fluorescent assays for detection and labeling.[13–16] First, the integration of fluorophores into polymeric assemblies and NPs has been recognized as one of the simplest strategies to enhance their solubility, while not only retaining the unique fluorescent properties of small molecule dyes, but also rendering them more structurally stable. Moreover, it has been well-established that the hydrophobic microenvironments of polymeric assemblies and NPs can typically enhance the quantum yields of certain fluorescent dyes, which usually possess relatively weak fluorescence emissions in polar organic solvents or aqueous media.[14,17–21] Furthermore, the polymeric matrix can endow the fluorometric system with additional sites for further functionalization and designing versatility, rendering possible the construction of multifunctional nanomaterials.

It is worth noting that tedious multistep synthetic procedures are typically required for small molecule-based FRET systems. However, since polymeric assemblies and NPs can be physically embedded or covalently labeled with two or more emitting fluorophores by employing nanosized polymeric assemblies or NPs as the scaffolds, the once challenging task of building sophisticated FRET systems has been rendered much easier.

CAS Key Laboratory of Soft Matter Chemistry, Department of Polymer Science and Engineering, Hefei National Laboratory for Physical Sciences at the Microscale, University of Science and Technology of China, Hefei, Anhui 230026, China. E-mail: sliu@ustc.edu.cn

Furthermore, the advent of the click chemistry concept[22–24] and well-developed controlled radical polymerization techniques,[25,26] such as nitroxide-mediated radical polymerization (NMP),[26,27] atom transfer radical polymerization (ATRP),[28,29] and reversible addition–fragmentation chain transfer (RAFT) polymerization,[30–32] has rendered possible the fine tuning of chemical compositions and morphologies of polymeric assemblies and NPs, leading to the precise spatial organization of multiple fluorophores.[33] Thus, polymeric assemblies and NPs have recently been frequently utilized to modulate the FRET processes.[34–38]

In addition to the use of polymeric assemblies and NPs as dye-immobilizing matrices, the incorporation of fluorescent moieties into stimuli-responsive polymeric assemblies and NPs represents a new trend in the application of the fluorescence technique for detection, imaging, and labeling purposes with integrated extra intriguing features.[13,14] It has been well-known that stimuli-responsive polymers are capable of exhibiting reversible or irreversible changes in physical properties and/or chemical structures to small changes in the external environment. Various types of stimuli, *e.g.*, pH, temperature, ionic strength, light irradiation, mechanical forces, electric, magnetic, and acoustic fields, specific analytes or external additives (ions, bioactive molecules, *etc.*) have been employed in a single or combined fashion to induce changes in chain conformation, solubility, surface charges, and morphologies of self-assembled aggregates.[14,39–51] It is also becoming apparent that stimuli-responsive fluorescent polymeric assemblies and NPs have several advantages over their small molecule analogues in terms of aqueous media dispersibility, photostability, emission switchability, biocompatibility, stimuli-responsiveness, and designing versatility.[14]

In the past five years, stimuli-responsive fluorescent polymeric assemblies and NPs have emerged to be an attractive and exciting research direction, which can be generally categorized into three main designing types: (1) lighting up fluorescence emission; (2) tuning fluorescence emission; (3) modulating FRET processes (see Scheme 1). These fascinating fluorescent polymeric assemblies and NPs offer unique and versatile platforms for diverse applications ranging from detection, imaging, bio-labeling, to optoelectronic systems. This feature article will focus on the recent developments of polymeric assemblies and NPs-based stimuli-responsive fluorescent systems and highlight their future practical applications with selected literature reports.

2. Lighting up fluorescence emission of polymeric assemblies and NPs

The lighting up of fluorescence emission is a process in which the fluorescence of latent moieties can be generated or switched on through selective chemical reactions or supramolecular recognition in the presence of one or more specific analytes, such as metal ions, proteins, pH variation, photo irradiation,

Changhua Li

Changhua Li was born in Anhui Province, China, in 1985. He received his BS degree in polymer materials and engineering from the University of Science and Technology of China in 2007. Since then he has been pursuing his PhD degree under the supervision of Prof. Shiyong Liu at the same institution. In 2010, he spent one year at the University of Mainz as exchange PhD student with Prof. Manfred Schmidt. His current research interest focuses on stimuli-responsive polymer-based functional materials.

Shiyong Liu

Shiyong Liu was born in Hubei Province, China, in 1972. He obtained his BS degree in 1993 and MS degree in 1996 from Wuhan University, majoring in environmental chemistry and polymer chemistry, respectively. After obtaining his PhD degree in 2000 at Fudan University under the supervision of Prof. Ming Jiang, he spent three and a half years at University of Sussex and University of Delaware as a postdoctoral fellow, working with Prof. Steven P. Armes (currently at University of Sheffield) and Prof. Eric W. Kaler (currently at University of Minnesota), respectively. Since 2004, he has been a professor of Polymer Science and Engineering at the University of Science and Technology of China. He is a recipient of 100 Talents Program (CAS, 2004), Distinguished Young Scholars Award (NSFC, 2004), Cheung Kong Professor Award (Ministry of Education of China, 2009). He served in the Editorial Advisory Board for Macromolecules (ACS, 2008–2010). He has served as the Head of Department of Polymer Science and Engineering since 2004 and the Director of CAS Key Laboratory of Soft Matter Chemistry since 2010. He has published over 160 peer-reviewed journal papers and 6 book chapters. As of Dec 2011, his works have been cited over 4300 times with an H-index of 38. His current research interest includes the design and synthesis of functional polymeric materials, colloids, and stimuli-responsive polymeric assemblies with controlled properties for applications in imaging, sensing, and nanomedicine.

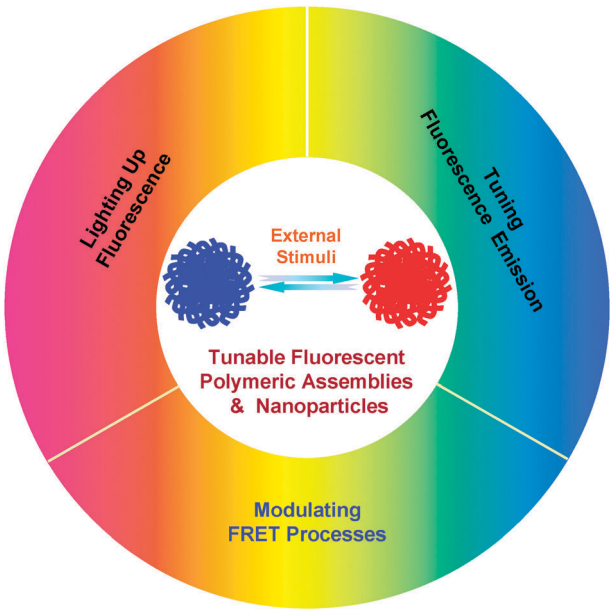

Scheme 1 Three main types of strategies employed in designing fluorescent polymeric assemblies and NPs with external stimuli-responsive emission characteristics: lighting up fluorescence, tuning fluorescence emission, and modulating FRET processes.

and target-specific functional moieties. Some recent efforts have been devoted to develop fluorogenic polymeric assemblies and NPs which possess broad applications in optical devices, analytical chemistry, and biological assays due to the high sensitivity and spatial resolution of fluorogenic processes. Some typical examples of fluorogenic polymeric assemblies and NPs are highlighted below.

2.1. Stimuli-triggered turn-on of fluorescence emission

Stimuli-triggered turn-on of fluorescence emission, also called fluorogenic process, of initially nonfluorescent polymeric assemblies and NPs can be achieved *via* selective chemical reactions. Rhodamine (RhB) is an orange-emitting fluorescent dye with high quantum yield. The fluorescence emission of RhB can be caged *via* chemical transformations when it is in the spirolactam form, and the subsequent external stimuli-induced ring-opening reaction leads to the formation of highly fluorescent acyclic form.[52–54] By taking advantage of the prominent emission off–on switchable characteristics of RhB derivatives, a variety of fluorescent chemosensors have been constructed from polymeric assemblies and NPs.[17,55–57] Recently, Hu *et al.*[55] integrated conventional thermo-responsive double hydrophilic block copolymers (DHBCs) with switchable RhB derivatives to fabricate fluorogenic polymeric micelles responsive to Hg^{2+} ions. By using a RAFT polymerization technique, they synthesized well-defined DHBCs of poly(ethylene oxide) and poly(*N*-isopropylacrylamide-*co*-RhBHA), PEO-*b*-P(NIPAM-*co*-RhBHA) with the RhB-based Hg^{2+}-reactive moieties (RhBHA) in the thermoresponsive PNIPAM block. Nonfluorescent RhBHA moieties are subjected to selective ring-opening reaction upon addition of Hg^{2+} ions, producing highly fluorescent acyclic RhB moieties. Due to the excellent dispersibility and stability of RhBHA-functionalized DHBC micelles in aqueous media, water-soluble fluorometric Hg^{2+} probes were constructed with prominent detection performance. Moreover, the hydrophobic microenvironments within fluorogenic polymer micelles at elevated temperatures considerably enhanced the detection sensitivity of Hg^{2+} ions as compared to that of block copolymer unimers at room temperature. Recently, a similar strategy was also employed to construct dual fluorescent chemosensors for Zn^{2+} ions and temperature in purely aqueous media.[58]

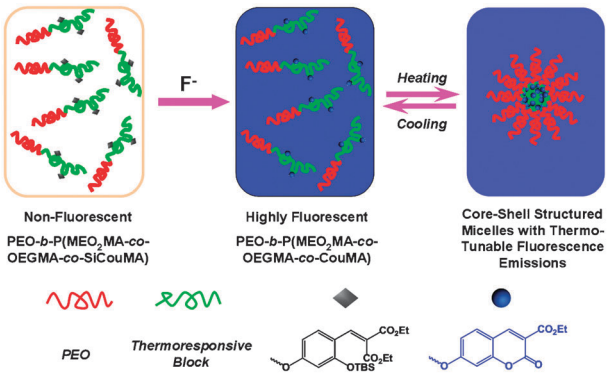

Fig. 1 Schematic illustration for the fabrication responsive DHBC-based highly selective and sensitive fluorescence turn-on probes for fluoride ions working in purely aqueous media by exploiting fluoride ions-induced cyclization reaction of non-fluorescent moieties to induce the formation of fluorescent coumarin moieties within the thermo-responsive block. Reproduced with permission from ref. 59. Copyright 2011 American Chemical Society.

Recently, Jiang *et al.*[59] reported a novel type of highly selective and sensitive fluorescence "turn-on" reactive probes for fluoride ions (F^-) in purely aqueous media based on functionalized DHBCs (Fig. 1). Through RAFT polymerization and post-modification, they grafted fluoride ion-reactive coumarin derivatives to the thermo-responsive diblock copolymer, PEO-*b*-P(MEO_2MA-*co*-OEGMA-*co*-SiCouMA), where MEO_2MA and OEGMA are di(ethylene glycol) monomethyl ether methacrylate and oligo(ethylene glycol) monomethyl ether methacrylate (M_n = 475 Da, mean degree of polymerization, DP, is 8–9), respectively. In the presence of F^- ions, deprotection of non-fluorescent SiCouMA moieties by F^- ions followed by spontaneous cyclization reaction leads to the formation of highly fluorescent coumarin residues (CouMA). Thus, PEO-*b*-P(MEO_2MA-*co*-OEGMA-*co*-SiCouMA) diblock copolymers can serve as highly efficient and selective fluorescence "turn-on" reaction probes for F^- ions in aqueous media. Interestingly, upon complete transformation of non-fluorescent SiCouMA moieties into fluorescent CouMA, the emission intensity of diblock copolymer solution decreases linearly with temperatures in the range of 20–60 °C, allowing its further application as a fluorometric thermometer. This work represents the first example of F^- ion-reactive polymeric probes working in purely aqueous media, which are capable of highly sensitive and selective fluorescent F^- sensing in the form of both unimers and polymeric micellar NPs.

In the past few decades, photochromic materials have attracted ever-increasing attention due to their promising application in data storage, optical switching, chemical sensing, and biological imaging.[60–63] As a typical example of

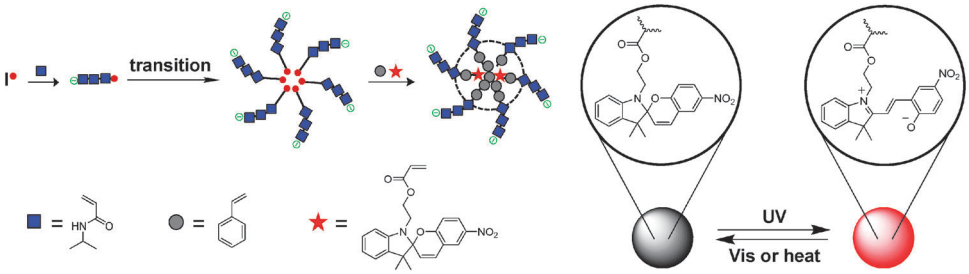

Fig. 2 Synthesis of spiropyran (SP)-embedded polymeric NPs *via* emulsion polymerization and the proposed SP–MC transition upon UV irradiation. Reproduced with permission from ref. 64 (Copyright 2006 American Chemical Society).

photochromic compound, spiropyran undergoes photo-induced reversible isomerization between non-fluorescent spiropyran (SP) and red-emitting fluorescent merocyanine (MC).[62,64–66] However, the fluorescence emission of MC is rather weak when molecularly dissolved in aqueous media or polar organic solvents. Zhu *et al.*[64] reported the synthesis of photo-induced fluorogenic polymeric NPs with SP moieties covalently labeled into the hydrophobic interior *via* emulsion polymerization (Fig. 2). The fluorogenic process from non-fluorescent SP form to red-emitting MC form is very fast and can be accomplished within ~10 s under UV irradiation. They found that upon UV irradiation, the fluorescence emission intensity of hydrophobic polymeric NPs covalently embedded with MC residues is at least 200 times higher than that of MC residues in the molecularly dissolved state. This is actually an aggregation-induced (enhanced) emission (AIE or AIEE) process as originated by Tang *et al.* in 2001.[67–70] In addition, the immobilization of SP moieties within hydrophobic NPs can considerably enhance the photostability. It should be noted that the fluorogenic process was only switched on upon UV irradiation, which will also spontaneously revert back to the non-fluorescent SP form under visible light irradiation or in a thermally controlled manner. This poses severe limitations for cellular imaging purposes considering UV absorption-related photo-damage. Very recently, they further demonstrated that 780 nm near infrared (NIR) two-photon irradiation can also induce the SP–MC transition within polymeric NPs and effectively switch on red fluorescence emission.[65] In comparison with the single-photon UV irradiation, two-photon NIR irradiation can potentially reduce photo-damage to living systems.

Fluorogenic click reaction has recently emerged as another powerful tool for imaging and detection applications by taking advantage of the high efficiency and specificity of click reactions and the distinct fluorescence emission properties of the click products.[71–79] In a typical fluorogenic click reaction, non-fluorescent alkyne- and azide-containing starting materials can be covalently coupled together to afford a highly fluorescent product (Fig. 3).[72] Original examples of fluorogenic click reaction were based on coumarin derivatives and were independently reported by the Wang[72] and Fahrni[73] research groups. Wooley *et al.*[74] utilized the fluorogenic click reaction to evaluate the availability of alkynyl functionalities within the core of shell cross-linked (SCL) block copolymer micelles on the basis of azide-functionalized coumarin, 3-azidocoumarin. They synthesized amphiphilic block copolymers with alkynyl moieties covalently attached to the hydrophobic block *via* RAFT polymerization. The self-assembly of these amphiphilic block copolymers in aqueous media followed by shell cross-linking afforded SCL micelles bearing alkyl groups within the core domain. The reactivity and availability of alkynyl functionalities were successfully evaluated *via* fluorogenic click reaction with 3-azidocoumarin. Based on the same principle, fluorogenic click reaction was also employed to evaluate the reactivity of alkynyl or azide moieties on the surface of polymeric NPs[75,76] and to monitor the completeness of the protein–polymer conjugation process.[77]

Since Cu(I) is an indispensible catalyst during the click reaction, O'Reilly *et al.*[78] recently utilized the fluorogenic click reaction to investigate the catalytic activity of a Cu(I)/terpyridine complex within SCL polymeric micelles. They synthesized amphiphilic block copolymers bearing terpyridine moieties in the hydrophobic block *via* NMP. The amphiphilic copolymers self-assembled into spherical micelles and were cross-linked in the shell layer to afford SCL micelles with terpyridine moieties located in the hydrophobic core. After forming the Cu(I)–terpyridine complex within SCL micelles, the fluorogenic click reaction between non-fluorescent phenylethynyl and 3-azidocoumarin was then conducted in the presence of SCL micelles. The availability and catalytic activity of terpyridine moieties, after complexation with Cu(I), can then be quantified on the basis of the fluorescence emission intensities.

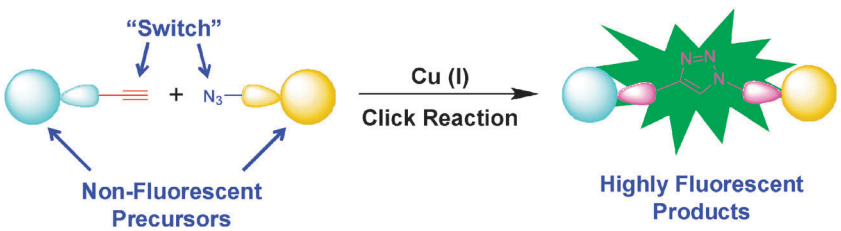

Fig. 3 Schematic representation of a typical fluorogenic click reaction. Reproduced with permission from ref. 72. Copyright 2010 The Royal Society of Chemistry.

2.2. Stimuli-activatable fluorescence recovery

It should be noted that in the above examples of fluorogenic polymeric assemblies and NPs, the changes in chemical structure in the latent fluorescent moieties are necessary to turn on the fluorescence emission. Apart from this, there is another type of fluorescence turn on process in which the initially quenched fluorescence emission can be recovered through a stimuli-triggered dequenching process. In a typical example, Kim *et al.*[80] reported a novel type of activatable fluorogenic probe based on the polymeric NPs platform (Fig. 4). The initially strongly quenched fluorogenic probe consists of NIR dye (Cy5.5) and the NIR dark quencher (BHQ-312), and they are connected together by a matrix metalloproteinase (MMP)-specific peptide sequence. The peptide-based probe was then covalently attached onto the surface of self-assembled chitosan NPs, which endows the enzymatic fluorogenic system with tumor-homing specificity and *in vivo* sensitivity by taking advantage of the enhanced permeability and retention (EPR) effect of polymeric NPs. The multiple attachment of the peptide probe onto polymeric NPs also incurs the extra NIR dye–dye self-quenching effect. When the polymeric NP-based fluorogenic system is exposed to the specific MMP of interest, pronounced fluorescence emission recovery of Cy5.5 was then achieved due to the enzymatic cleavage of peptide linkage between Cy5.5 and the quencher (BHQ-312). The above described system was also successfully applied for *in vivo* optical tumor imaging.

In a similar study, Nagasaki *et al.*[81] developed a type of biocompatible and caspase-3-specific PEGylated polymer nanogels for probing the apoptosis process during cancer chemotherapy. They designed PEGylated polyamine nanogels with gold nanoparticles (AuNPs) in the core as dark quenchers and fluorescein isothiocyanate (FITC)-labeled Asp-Glu-Val-Asp (DEVD) peptides at the tethered PEG chain ends. The PEGylated nanogels consist of crosslinked pH-responsive poly[2-(*N*,*N*-diethylamino)ethyl methacrylate] (PDEAEMA) cores and surface tethered PEG chains bearing free carboxylic acid or acetal terminal groups for the covalent attachment of tumor-specific ligands. Initially the fluorescence of FITC was quenched by AuNPs in the absence of caspase-3, whereas pronounced fluorescence signals were recovered upon addition of caspase-3 owing to the cleavage of the DEVD peptide sequence by activated caspase-3. Since caspase-3 plays an important role in cell apoptosis and will be present in apoptotic cells, the reported caspase-3-activatable fluorogenic nanoprobe can be utilized for high-resolution apoptosis imaging and real-time monitoring of tumor responses to chemotherapy.

Gianneschi *et al.*[82] reported the utilization of DNA-brush copolymer micelles as fluorogenic substrates for detection and signal amplification *via* DNAzyme-mediated cleavage reactions of single-stranded DNA (ssDNA). They designed a DNA substrate possessing two sequences complementary to the recognition portions of the DNAzyme on either side of the cut-site, and a fluorescein moiety was incorporated at the 3′-termini of the strand. The DNA-brush copolymer was synthesized *via* post-modification of a well-defined block copolymer with a 5′-amino-modified DNA substrate. The resulting DNA-brush copolymer self-assembled into spherical DNA/polymer hybrid micelles of ~20 nm in diameter. Initially, the active site of DNAzyme was blocked due to hybridization with its inhibitor (DNA-Inh). Upon addition of target DNA sequence (DNA-T), DNA-T rapidly invades into the inhibited DNAzyme duplex, releasing active DNAzyme. Substrate DNA-brush copolymer micelles were then added to the solution of activated DNAzyme, resulting in highly fluorescent emission due to the cleavage of DNA linkages at the core–shell interface. The key benefit of the reported hybrid polymeric assemblies over materials simply decorated with DNA is that the substrate DNA is densely grafted, leading to considerably enhanced detection sensitivity even at the picomolar level.

2.3. Aggregation-induced emission (AIE)

Aggregation-induced emission (AIE) is another fluorogenic process of emerging importance in which non-fluorescent dyes in the molecularly dissolved state in solution can be rendered

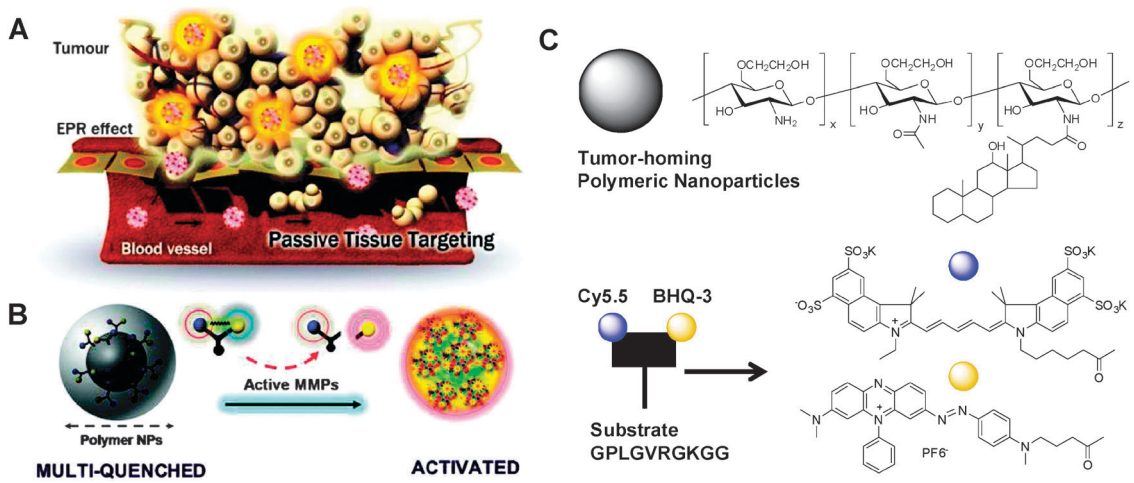

Fig. 4 (A) Schematic illustration of the MMP-specific polymeric nanoparticle based optical nanosensor (NS). When MMPs meet the NS at the site of disease, cleavage of the fluorogenic peptide occurs owing to specific substrate recognition by the MMPs, affording pronounced NIR fluorescence signal recovery due to dequenching of the dye (Cy5.5). (B) MMP-specific NS. After cleavage of the peptide substrate by MMPs, NIR fluorescence dyes are released from NPs and fluoresce brightly. (C) Chemical structures of polymeric NPs and MMP-sensitive fluorogenic peptide. Reproduced with permission from ref. 80. Copyright 2010 The American Chemical Society.

highly emissive *via* aggregation or absorbing onto bulky substrates.[67,69,70] Tang *et al.* discovered the AIE phenomenon in 2001, which is in stark contrast to the notorious aggregation-induced quenching phenomenon typically encountered for conventional small molecule dyes.

By combining the lower critical solution temperature (LCST) phase transition behavior of PNIPAM chains, Tang *et al.*[83] recently designed a novel type of AIE-based fluorogenic thermometer. They synthesized AIE dye-labeled PNIPAM, P(NIPAM-*co*-TPE), *via* the copolymerization of NIPAM with a tetraphenylethene (TPE)-containing monomer which exhibits the AIE characteristics.[84] Initially, the THF solution of P(NIPAM-*co*-TPE) is non-emissive, whereas increase in contents of water, a poor solvent for TPE, led to enhanced fluorescence emission due to the aggregation process. Interestingly, heating the aqueous solution of P(NIPAM-*co*-TPE) nanoparticle dispersion above its LCST can further lead to $\sim$2 times increase in fluorescence intensity due to more prominent aggregation of P(NIPAM-*co*-TPE) chains at elevated temperatures. Thus, P(NIPAM-*co*-TPE) can act as a fluorogenic thermal probe that reveals delicate details concerning the thermal phase transition of PNIPAM, which are generally inaccessible by other analytical techniques. On the other hand, it is well-known that amphiphilic molecules can self-assemble into well-organized nanostructures such as micellar aggregates above the critical micelle concentration (CMC) to afford hydrophobic interiors which can induce the emission of AIE dyes. Based on this principle, Tang *et al.* successfully evaluated the CMC of a model biomacromolecule (lecithin).[85]

Very recently, we designed a novel type of water-soluble charge-generation polymers (termed as CGPs) possessing pendent carbamate-masked amine functionalities, which can undergo stimuli-triggered transition from the initially neutral state to the charged one in the presence of a specific analyte of interest.[86] The charge-generation process was coupled with the induced aggregation of TPE derivatives bearing four carboxyl acid moieties (TPE–$COOH_4$) to design reliable, cost-effective, quantitative, and sensitive aqueous-based fluorogenic probes (Fig. 5).[87] The presence of specific analytes of interest, H_2O_2 or thiols, can trigger the transformation of CGPs from the initially uncharged state into a cationic polyelectrolyte *via* the chemoselective cleavage of carbamate protecting functionalities. This will release primary amine residues and induce the aggregation of negatively charged TPE–$COOH_4$, leading to the dramatic enhancement of fluorescence emission.

3. Tuning fluorescence emission

Apart from the three main types of fluorogenic or emission off–on switchable polymeric assemblies or NPs described in the previous section, considerable attention has also been paid to fluorescent polymeric assemblies and NPs possessing stimuli-tunable emission intensities. The features of tunable fluorescence emissions mainly arise from the intrinsic properties of the attached fluorescent dyes or the responsiveness of polymer matrices or a combination of them. Typical examples of intensity-tunable fluorescent polymeric assemblies and NPs are highlighted below.

3.1. Fluorescent polymeric assemblies and NPs attached with stimuli-sensitive dyes

A general strategy for the construction of stimuli-tunable fluorescent polymeric assemblies and NPs employs inert polymer matrices functionalized with stimuli-sensitive dyes. Fluorescein is one of the most well-known pH-sensitive dyes. It possesses a pK_a of $\sim$5.6 and exhibits pH-switchable transformation between mono- and di-anionic states.[88] Sun *et al.*[89] reported the fabrication of poly(acrylamide) (PAM) nanogels-based ratiometric pH probes *via* covalent functionalization with a fluorometric pH-indicating fluorescein dye and pH-insensitive RhB as the reference dye. Thus, the ratiometric fluorescent

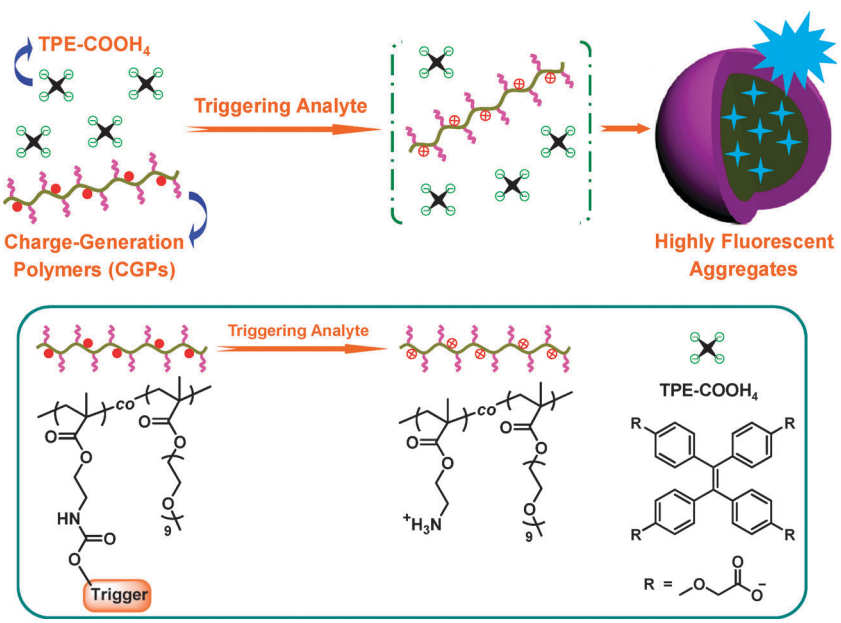

Fig. 5 Construction of fluorogenic sensors *via* the integration of negatively charged AIE-active fluorogens (TPE–$COOH_4$) with water-soluble amine-caged charge-generation polymers (CGPs) exhibiting selective and specific analyte-triggered switching from the initially uncharged state to cationic polyelectrolytes. Reproduced with permission from ref. 87. Copyright 2011 Wiley-VCH.

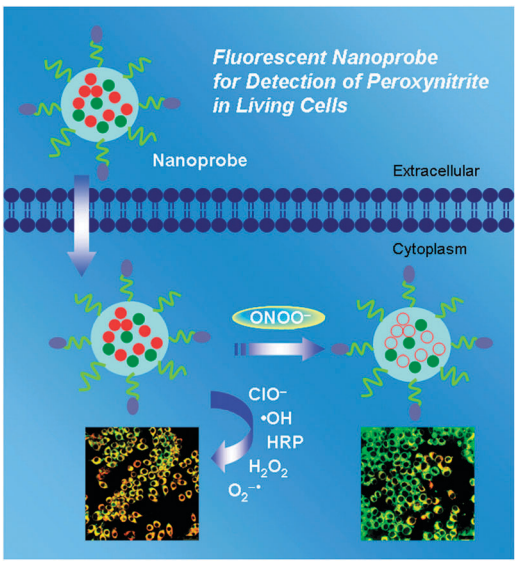

Fig. 6 A highly selective cell-permeable polymeric micelles-based fluorescent nanoprobe for the ratiometric detection and imaging of peroxynitrite within living cells. Reproduced with permission from ref. 92. Copyright 2011 Wiley-VCH.

pH-reporting is possible based on dual dye-labeled nanogels. Similar ratiometric pH sensors based on other inert polymer matrices such as polystyrene NPs[90] and biocompatible dextran NPs[91] were also reported. These polymeric NP-based ratiometric pH probes hold promising applications in diagnosing certain cancer diseases and investigating cellular internalization pathways.

Very recently, Tang *et al.*[92] developed a novel type of polymeric micelle-based fluorescent probes with the surface decorated with cell-penetrating peptide sequences. The micellar interior contains $ONOO^-$-reactive indicator dye (BzSe-Cy) and a reference dye (IRhB) for the ratiometric detection and imaging of $ONOO^-$ (Fig. 6). The small molecular BzSe-Cy probe is specific for $ONOO^-$ and the selectivity can be further improved by encapsulating BzSe-Cy within polymeric NPs. In the presence of $ONOO^-$, BzSe-Cy was oxidized, which was accompanied with a significant decrease in fluorescence emission; whereas the fluorescence emission of IRhB did not change. This leads to the highly selective ratiometric detection of $ONOO^-$. Additional experiments demonstrate that the novel type of polymeric micelles-based biosensor possesses unique advantages of excellent water solubility, photostability, biocompatibility, and NIR excitation and emission. Furthermore, ratiometric fluorescence imaging in living cells confirmed effective cell permeability and capability of visualizing intracellular $ONOO^-$ levels.

Chen *et al.*[93] recently designed a new strategy to fabricate fluorescent polymeric NPs responsive to a variety of metal ions. They utilized propargyl bromide (PB) to cross-link polystyrene-*b*-poly(4-vinylpyridine), PS-*b*-P4VP, a diblock copolymer in DMF, affording core cross-linked polymeric NPs. PB first quaternized pendent pyridine residues in the P4VP block, and the grafted propargyl moieties were then activated and polymerized to afford structurally stable NPs stabilized by PS coronas. The resulting conjugated polyacetylene oligomer sequences within NP cores endow polymeric NPs with high fluorescence emission. Interestingly, the fluorescent core cross-linked NPs are very sensitive to the addition of metal ions with modulated emission intensities.

3.2. Stimuli-tunable fluorescence emission due to responsive polymer matrix

It has been well-established that microenvironments around fluorescent dyes play an important role in the determination of quantum yields.[14,17–21] Typically, stimuli-responsive polymers undergo reversible or irreversible changes in physical properties and/or chemical structures to external stimuli, accompanied with changes in chain conformation and hydrophobicity/hydrophilicity.[39–43] Thus, upon incorporating fluorescent dyes into responsive polymer matrices, external stimulus can be converted into fluorescence signals due to changes in properties of surrounding microenvironments.

In 2003, Uchiyama *et al.*[94] reported a nice example of polymer-based fluorescent thermometer by taking advantage of the effect that the quantum yields of polarity-sensitive fluorescent dyes can be dramatically enhanced within hydrophobic microenvironments when polymer chains are subjected to thermo-induced aggregate formation. Up to now, Uchiyama *et al.*[94–101] have developed a variety of polarity-sensitive fluorescent reporters based on benzoxadiazole motifs including 4-*N*-(2-acryloyloxyethyl)-*N*-methylamino-7-*N*,*N*-dimethylaminosulfonyl-2,1,3-benzoxadiazole (DBDAE) and 4-(2-acryloyloxyethylamino)-7-nitro-2,1,3-benzoxa-diazole (NBDAE). In a typical example, they developed dual fluorescent sensors for pH and temperature based on DBDAE-labeled thermo- and pH-responsive polymers (Fig. 7).[95] On the basis of DBDAE dye-labeled thermo-responsive PNIPAM microgels, they also prepared polymeric NP-based fluorescent thermometers exhibiting accurate temperature detection capability ($\sim$0.5 °C resolution) in the presence of increasing KCl concentrations (0–100 mM).[101] Additionally, this novel type of polymeric NP-based thermometer can be employed for intracellular thermometry. Inspired by Uchiyama's work, Stuart *et al.*[102] designed an intracellular ratiometric fluorescent thermometer based on core cross-linked micelles covalently functionalized with a polarity-sensitive probe (HMA) in micellar cores and reference dye (TRITC) at micellar coronas. Quite recently, Schubert and Hoogenboom *et al.*[103,104] developed two novel types of fluorescent thermometers based on pyrene-labeled thermoresponsive polymers.

In another example, Chen *et al.*[105] covalently labeled polarity-sensitive fluorescent dye, 3-hydroxyflavone (3-HF), into thermo-responsive PNIPAM nanogels to achieve ratiometric fluorescent detection of temperature (Fig. 8). 3-HF displays dual-band emissions associated with normal excited state intramolecular charge transfer (ESICT) and tautomer excited state intramolecular proton transfer (ESIPT).[106–109] 3-HF exhibits greenish fluorescence emission in aprotic solvents originating from the coupled ESICT/ESIPT processes, whereas in highly polar or protic solvents, the ESIPT reaction is suppressed, resulting in blue fluorescence emission. Based on this distinctive property, 3-HF labeled PNIPAM nanogels with ratiometric temperature read-out capability were synthesized.

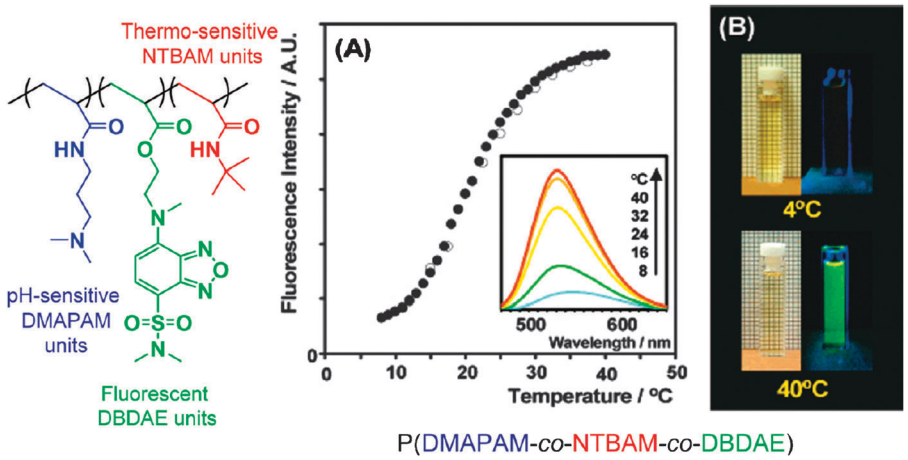

Fig. 7 Thermo-responsive P(DMAPAM-*co*-NTBAM-*co*-DBDAE) copolymer in aqueous solution serves as a fluorescent molecular thermometer. (A) Fluorescence intensity changes upon heating and cooling cycles. Inset: fluorescence emission spectra. (B) Visual and fluorescent images recorded at temperatures below and above the LCST. Reproduced with permission from ref. 95. Copyright 2004 American Chemical Society.

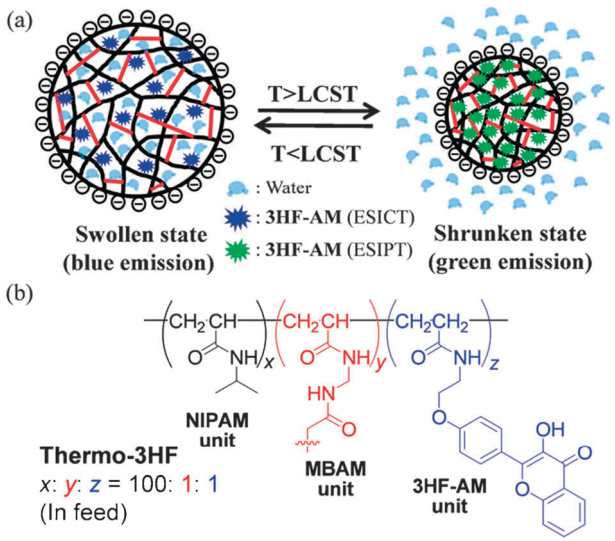

Fig. 8 (a) 3-HF-labeled nanogels in the swollen state emit blue fluorescence in aqueous media; whereas when the local temperature exceeds the LCST, nanogels shrink accompanied with prominent green emission. (b) The chemical compositions of 3-HF-labeled thermo-responsive polymeric nanogels. Reproduced with permission from ref. 105. Copyright 2011 The Royal Society of Chemistry.

Within the temperature range of 33–41 °C, the emission color of thermo-responsive nanogels changes from blue to green, associated with the change in ratiometric magnitude of ~8.7-fold.

It has been recognized that ultra small Ag nanoparticles (Ag NPs) can emit strong and nonbleaching fluorescence.[110] Recently, Zhou *et al.*[111] introduced fluorescent Ag NPs into glucose-responsive polymeric nanogels to fabricate fluorescent glucose sensors. SDS-capped Ag NPs (10 ± 3 nm) were synthesized first. The subsequent free-radical precipitation polymerization in the presence of Ag NPs afforded a glucose-responsive gel layer of poly(4-vinylphenylboronic acid-*co*-2-(dimethylamino)ethyl acrylate), P(VPBA-DMAEA), at the surface of Ag NP templates. For the obtained hybrid fluorescent polymeric nanogels, the fluorescence of Ag NPs is gradually quenched when the copolymer gel layer gradually swells at elevated glucose concentrations. It should be noted that the fluorescence emission of free Ag NPs is almost independent of glucose in the tested concentration range of 0–30 mM. Changes in local refractive index of the gel medium surrounding Ag NPs during glucose-induced volume phase transition of the gel layer are responsible for the modulation of fluorescence emission. This is due to the generation of negative charges resulting from the binding of glucose with VPBA to form cyclic boronate linkages; correspondingly, the pK_a of VPBA residues decreases, leading to the shift of hydrophilic/hydrophobic balance. Based on this concept, Hoogenboom *et al.*[112] recently also designed a novel fluorescent sugar sensor based on solvatochromic fluorescent dye (TBTS)-labeled PVPBA.

In a recent example, Gao *et al.*[113] ingeniously invented a series of tunable and pH-activatable micellar NPs based on the supramolecular self-assembly of dye-labeled pH-responsive diblock copolymer (Fig. 9). They synthesized two series of block copolymers (PEO-*b*-PR) consisting of poly(ethylene oxide) (PEO) and tertiary amine-containing PR blocks by ATRP. The PR blocks were covalently labeled with fluorescent dyes possessing low Stokes shift. At pH > pK_a of the PR block, the diblock copolymers self-assemble into micelles with the PR block forming micellar cores, leading to quenching of fluorophores by combined homo-FRET and PET mechanisms. Upon pH decrease (pH < pK_a), micellar to unimer transition occurs accompanied with dramatic increase in fluorescence emission intensities. The reported pH-activatable fluorescent micellar NPs possess tunable and ultrasensitive pH responses under physiological and intracellular conditions (5.0–7.4). These polymeric NPs possess fast temporal response (<5 ms), large increase of emission intensity between on and off states (up to ~55 times), and require a change of only less than 0.25 pH units for effective fluorescence turn-on.

3.3. Combined effects of responsive polymer matrix and stimuli-sensitive dyes

The combination of a stimuli-responsive polymeric matrix with the labeling of stimuli-sensitive fluorescent dyes can endow the sensing system with multi-functionality and enhanced emission tunability.

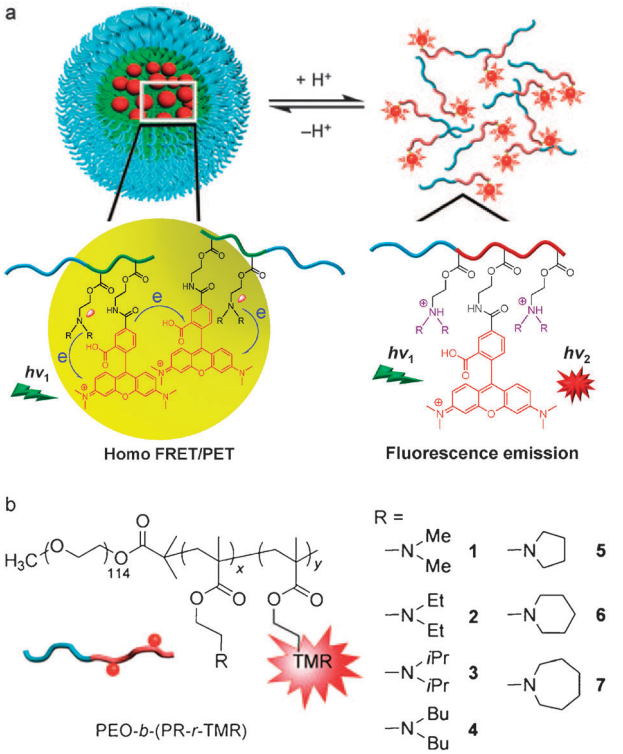

Fig. 9 (a) Schematic design of pH-switchable micellar fluorescent nanoprobes. (b) Structures of PEO-*b*-(PR-*r*-TMR) diblock copolymers (dialkyl and cyclic series). Reproduced with permission from ref. 113. Copyright 2011 Wiley-VCH.

In a recent example, Zhou *et al.*[114] reported the synthesis of pH and H_2O_2 dually responsive fluorescent microgels by covalently labeling H_2O_2-sensitive dyes (Calcon) into pH-responsive poly(NIPAM-acrylic acid-acrylamide), P(NIPAM-*co*-AA-*co*-AAm), microgels. The PAA segments within microgels were incorporated for endowing pH responsiveness sensitivity and PAAm segments were for directing the highly ordered assembly of dye molecules. The pH-induced shrinkage of polymeric microgels resulted in a systematic blue shift of emission bands and dramatically enhanced emission intensity due to changes in delocalized electron systems of Calcon domains. The fluorescent microgels also exhibit highly sensitive H_2O_2-induced fluorescence quenching and *in vivo* optical imaging can be achieved.

In another notable example, Zhang *et al.*[115] reported the fabrication of thermo- and pH-sensitive multicolor polymeric micelles based on thermoresponsive block copolymers covalently labeled with fluorescent Eu(III) complexes, $Eu(DBM)_3$, and pH-sensitive fluorophores, FITC. The green-emitting dye, FITC, and red-emitting dye, $Eu(DBM)_3$, were, respectively, and covalently attached to P(NIPAM-*co*-HEMA)-*b*-P4VP and P(NIPAM-*co*-EIPPMMA)-*b*-PVPh diblock copolymers. These two types of amphiphilic block copolymers can self-assemble to form mixed micelles in aqueous solution *via* hydrogen bonding interactions between PVPh and P4VP. The emission properties of the resulting micellar complexes can be dually controlled by temperature and pH changes. At 25 °C, the fluorescence intensity of pH-sensitive FITC increases with increasing pH, while the fluorescence of $Eu(DBM)_3$ moieties is almost irrespective of solution pH. When the temperature increases from 15 to 45 °C with pH fixed at 7.0, the fluorescence of $Eu(DBM)_3$ decreases with an increase in temperature, whereas the FITC fluorescence exhibits negligible change. This is due to that the $Eu(DBM)_3$-labeled P(NIPAM-*co*-EIPPMMA) block collapsed at elevated temperature, and $Eu(DBM)_3$ fluorophores were entrapped into NP cores, leading to the excitation of $Eu(DBM)_3$ fluorophores being shielded by the shell of micellar complexes; whereas the FITC-labeled P(NIPAM-*co*-HEMA) block did not exhibit similar thermo-induced phase transition due to the hydrophilicity of HEMA units. These dually responsive multicolor fluorescent polymeric micelles can serve as pH and temperature sensors.

Very recently, we designed thermoresponsive nanogel-based dual fluorescent sensors for temperature and Hg^{2+}.[116] We prepared novel 1,8-naphthalimide-based polarity-sensitive and Hg^{2+}-reactive fluorescent monomer (NPTUA)-labeled near-monodisperse thermoresponsive PNIPAM nanogels *via* emulsion polymerization (Fig. 10). At room temperature, the fluorescence of the nanogel blue shifted from 528 nm (green emission) to 482 nm (blue emission) upon addition of Hg^{2+} due to the Hg^{2+}-induced formation of imidazoline moieties within NPTUA. Upon heating above the volume phase transition (VPT) temperature, the fluorescence intensity of NPTUA-labeled nanogels in the absence of Hg^{2+} exhibits ~3.4-fold increase due to that NPTUA moieties are located in more hydrophobic microenvironments, which can enhance the quantum yields of NPTUA residues. Moreover, it was observed that the detection sensitivity to Hg^{2+} can be further improved above the nanogel phase transition temperature. A similar strategy has been utilized to detect Cu^{2+} with thermo-tunable detection sensitivity based on fluorescent phenanthroline (PhenUMA) moieties-labeled PNIPAM microgels.[117] Recently, Wan *et al.*[118] introduced another Hg^{2+}-reactive 1,8-naphthalimide-based derivative into thermo-responsive core cross-linked (CCL) polymeric micelles to construct dual fluorescent sensors for Hg^{2+} and temperature.

4. Modulating FRET processes

FRET is a nonradiative transfer process of the excitation energy from an excited donor to a proximal ground-state acceptor through long-range dipole–dipole interactions.[9] It has been well-recognized as a powerful photophysical tool and utilized as a spectroscopic technique in the past several decades. In a typical FRET process, the FRET acceptor dye absorbs energy at the emission wavelength range of the FRET donor dye and then reemits the energy in the form of fluorescence. However, the reemission is sometimes not necessary, such as in the case of dark quenching. The rate of energy transfer is highly sensitive to many factors, such as the extent of spectral overlap between the emission band of the FRET donor and the absorption band of the FRET acceptor, the relative dipole orientations of the two dyes, and, most importantly, the spatial separation distance between them. The FRET process usually occurs over distances of 1 to 10 nm. It has found a wide range of applications in analytical chemistry, optical materials, protein folding studies, and biological assays. Nanosized polymeric assemblies and NPs offer a distinct nanoplatform for FRET processes due to improved stability, versatility in structural control, and the possibility of precise

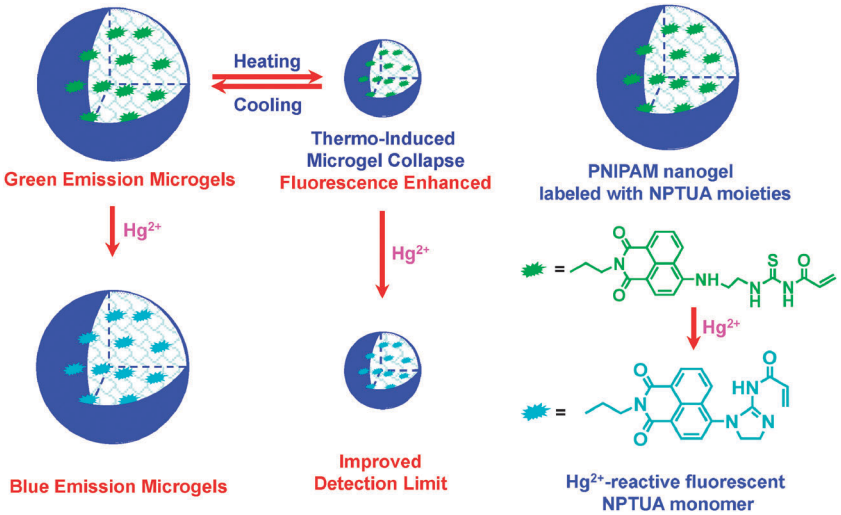

Fig. 10 The utilization of PNIPAM nanogels covalently labeled with NPTUA moieties as a ratiometric fluorescent sensor for Hg^{2+} ions with thermo-enhanced detection sensitivity due to thermo-induced collapse of thermo-responsive nanogels. Reproduced with permission from ref. 116. Copyright 2010 The Royal Society of Chemistry.

spatial organization of multiple fluorophores. Some typical examples of fluorescent polymeric assemblies and NPs with stimuli-tunable FRET processes are highlighted below.

4.1. Off–on switching of FRET processes

Stimuli-sensitive fluorescent dyes were widely used to modulate FRET processes within polymeric assemblies and NPs, as their spectroscopic properties can be facilely switched between two states upon the action of external stimuli. In a typical example, Zhu *et al.*[119] reported the construction of reversibly photoswitchable dual-color fluorescent polymeric NPs covalently labeled with perylene and photo-induced fluorogenic SP moieties as FRET donors and latent acceptors, respectively. Under visible light irradiation, SP moieties are in the colorless ring-closed spirolactam form, whereas perylene fluorophores located in the hydrophobic core strongly emit distinctive green fluorescence with high quantum yield. Upon UV irradiation, SP converts to the colored ring-opened MC form with the absorbance band overlapping well with the perylene emission bands, and this results in the turn-on of the FRET process from perylene to MC. Consequently, the characteristic green fluorescence from perylene was significantly quenched, whereas a new red-emitting band ascribing to the FRET acceptor (ring-opened MC moieties) occurs. The FRET process can be facilely switched off upon visible light irradiation, leading to the recovery of green fluorescence emission. It should be noted that the FRET process between perylene and SP with polymeric NPs can be reversibly switched on/off *via* alternate UV/visible light irradiation. Moreover, the off–on switching can be repeated many times without any apparent fatigue effects or photobleaching owing to the protection of the polymeric NP matrix. This novel type of high-contrast photoswitchable dual color fluorescent polymeric NPs might find promising applications for bioimaging and biosensing purposes.

Based on SP moieties, Zeng and Wu *et al.*[120–123] reported the design of other types of photoswitchable dual-color fluorescent polymeric assemblies and NPs. In a typical example, they employed nanosized ABC triblock copolymer micelles as a novel scaffold for modulating FRET processes (Fig. 11).[122]

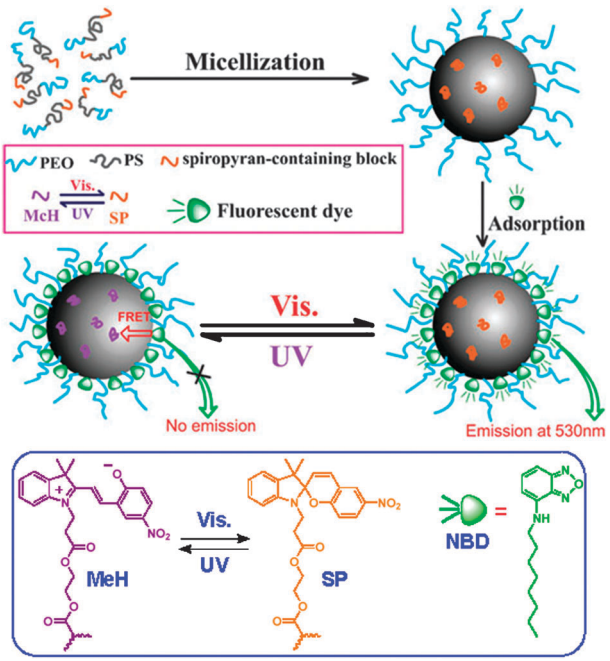

Fig. 11 Photoreversible fluorescence modulation of triblock copolymer micelle physically and covalently labeled with NBD and SP, respectively. The FRET process between NBD and SP can be switched on/off *via* alternate UV/Vis irradiation. Reproduced with permission from ref. 122. Copyright 2008 The Royal Society of Chemistry.

The consecutive ATRP of styrene and SP-based monomers by using a PEO-based macroinitiator leads to amphiphilic ABC triblock copolymers covalently labeled with SP. In aqueous solution, the triblock copolymer self-assembles into micelles with latent FRET acceptors, SP moieties, located in hydrophobic cores. To form FRET-based donor–acceptor pairs within polymeric micelles, the donor dye, a nitrobenzoxadiazolyl (NBD) derivative with a 8-carbon alkyl tail, was incorporated into micelles *via* hydrophobic interactions. Then, the FRET process between NBD and SP within polymeric micelles can be

reversibly switched on/off *via* UV or visible light irradiation. Very recently, Yildiz *et al.*[124] reported biocompatible and photoswitchable fluorescent polymeric assemblies based on the combination of boron dipyrromethene (BODIPY) and SP dyes.

Multicolor fluorescent polymeric assemblies and NPs exhibiting metal ion-switchable FRET processes have also been reported by utilizing metal ion-reactive fluorophores as potential FRET acceptors. In a recent example, Ma *et al.*[125] reported a facile strategy to construct a FRET-based ratiometric chemosensor for Fe^{3+} ions in aqueous media by using nanosized PEO-*b*-PS micelles as the scaffold. They designed a novel Fe^{3+}-reactive RhB derivative (SRhB-OH) for which the fluorescence emission can be selectively switched on *via* Fe^{3+}-induced ring-opening reaction. In their work, the FRET donor, NBD derivative, was incorporated into hydrophobic micellar cores during micelle formation, and the potential FRET acceptor, SRhB-OH, was then physically 'adsorbed' onto the micelle core/corona interface. Thus, the FRET donor and acceptor were physically segregated and kept within the effective energy transfer distance, the FRET process can be turned on upon addition of Fe^{3+} ions. The key to successful construction of the Fe^{3+} turn-on FRET system is that donors and acceptors can reside in appropriate positions within micelles as diblock copolymer micelles consist of low polarity cores and higher polarity coronas. However, the irreversible feature of the sensing strategy might limit its real applications.

It should be noted that in the above examples, when the FRET process was turned on, the characteristic fluorescence emission from donors was significantly quenched, accompanied with the appearance of a new fluorescence emission band ascribing to FRET acceptors. However, if the potential acceptor is just a quencher, the FRET process would only quench the emission of FRET donors without generating any new emission band. In a typical example, Chen *et al.*[126] developed a FRET-based Cu^{2+} fluorescent chemosensor based on core–shell polymeric NPs, which consist of poly(methyl methacrylate) (PMMA) cores embedded with Nile red and hydrophilic polyethyleneimine (PEI) coronas for high affinity Cu^{2+} binding. Upon addition of Cu^{2+}, the fluorescence emission is quenched due to FRET from Nile red to the newly generated Cu^{2+}/PEI complex at the NP surface. This biocompatible and sensitive fluorescent polymeric NP-based Cu^{2+} chemosensor might find practical applications for biosensing.

In a notable example, Larpent *et al.*[127] synthesized nanosized core–shell dual fluorescent cross-linked PS NPs surface attached with Cu^{2+}-selective ligands (cyclam) and physically embedded with two types of fluorophores, 9,10-diphenylanthracene (FRET donor) and pyrromethene PM567 (FRET acceptor), within NP cores. The donor and acceptor dyes were chosen to allow for the coupling of two FRET processes: (1) from the donor to the acceptor; (2) from encapsulated dyes to the Cu^{2+}–cyclam complex formed at the NP surface. Since the absorption bands of the Cu^{2+} complex overlap better with emission bands of FRET acceptors than those of donors, the FRET from acceptors (pyrromethene PM567) to the Cu^{2+} complex is more effective than that from donors. Thus, in this dual fluorescent polymeric NPs, the sensitized emission of acceptor dyes is efficiently attenuated whereas the remaining emission of donor dyes is much less affected, thus allowing for the detection of Cu^{2+} in a ratiometric manner upon excitation at a single (donor) wavelength. The close proximity between the encapsulated fluorophores and the surface grafted quencher-binding ligands imposed by the nanosized template results in large changes in FRET efficiencies upon Cu^{2+} binding. Owing to its design flexibility and modularity, the reported cascade FRET strategy based on dual fluorescent NPs holds great promise for the design of a variety of potent sensing devices.

4.2. Modulating FRET efficiency

For the examples described in the previous section concerning the off–on switching of FRET processes, polymeric assemblies and NPs were utilized as a scaffold for FRET donors and acceptors, and their nanosized dimensions can ensure FRET donors and acceptors within effective energy transfer distances. Besides, for certain polarity-sensitive fluorophores, the hydrophobic microenvironment within polymeric assembles and NPs can further help enhance the quantum yields. Recently, stimuli-responsive polymeric assemblies and NPs were also employed to modulate FRET efficiencies by tuning the spatial distance between FRET donors and acceptors *via* stimuli-induced collapse/swelling of the polymer matrix.

It has been well-established that thermoresponsive PNIPAM microgels exhibit thermo-induced swelling/collapse behavior in aqueous dispersion, *i.e.*, thermo-induced VPTs. Quantum dots (QDs) have been integrated into thermoresponsive PNIPAM microgels to construct thermal sensors by taking advantage of the unique emitting behavior of QDs,[128] *i.e.*, size-tunable emission color, narrow and symmetric emission profile, and high emission stability against photobleaching. In a typical example, Gong *et al.*[129] designed a FRET-based fluorescent thermometer on the basis of PNIPAM microgels with two types of CdTe QDs (with emission maxima being 520 and 610 nm, respectively) embedded into cores *via* hydrogen bonding interactions. The average spatial distance between CdTe QDs embedded into PNIPAM microgels is optimized to be larger than that required for effective FRET. Thus, thermo-induced collapse and swelling of PNIPAM microgels lead to tunable spatial distance between the two types of QDs and result in changes in FRET efficiencies.

Very recently, Ionov and Diez[130] reported a novel approach for tuning the LCST of PNIPAM copolymers *via* UV irradiation. In this approach, they incorporated hydrophobic photocleavable *o*-nitrobenzyl functionalities into PNIPAM chains. The random copolymer poly(NIPAM-*co*-*o*-nitrobenzyl acrylate), P(NIPAM-*co*-NBA), exhibits a lower LCST compared to that of the PNIPAM homopolymer prior to UV irradiation. Upon UV irradiation, the LCST of the P(NIPAM-*co*-NBA) copolymer increases due to the generation of the poly(NIPAM-*co*-acrylic acid) copolymer, P(NIPAM-*co*-AA). Inspired by Ionov's work, Yin *et al.*[131] recently reported the fabrication of thermo- and light-responsive P(NIPAM-DMNA-NBDAE-RhBEA) microgels consisting of NIPAM, photocleavable moieties, 5-(2-(dimethylamino)ethoxy)-2-nitrobenzyl acrylate (DMNA), FRET donors (NBDAE), and RhB-based FRET acceptors (RhBEA) *via* free radical emulsion polymerization (Fig. 12). Thermo-induced collapse and swelling of responsive microgels above and below VPT temperature, respectively, can finely tune the spatial proximity between NBDAE and RhBEA dyes, leading to the facile

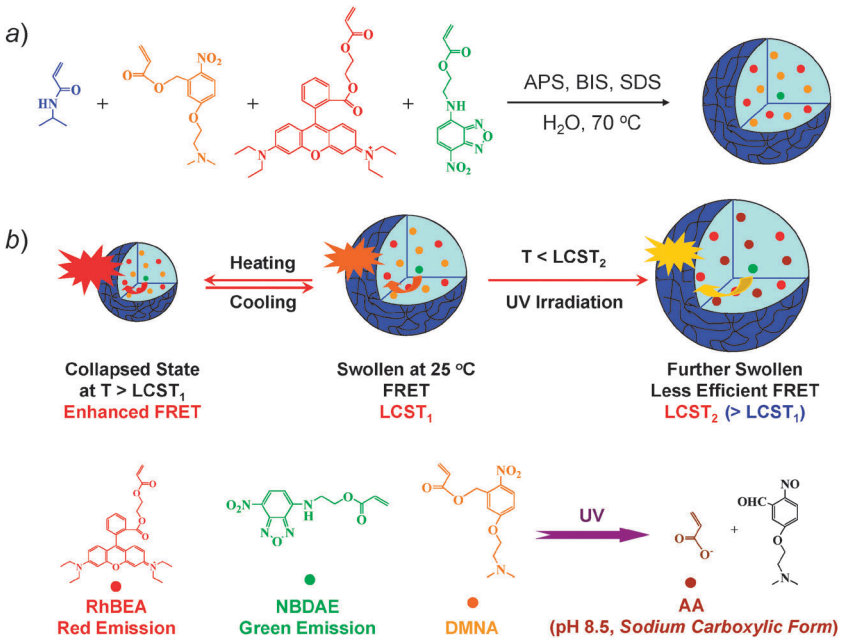

Fig. 12 (a) Synthetic schemes employed for the preparation of thermo- and photo-responsive P(NIPAM-DMNA-NBDAE-RhBEA) microgels *via* emulsion polymerization. (b) A schematic illustration of tuning the efficiency of FRET processes within P(NIPAM-DMNA-NBDAE-RhBEA) microgels by temperature, UV irradiation, or a combination of them. Reproduced with permission from ref. 131. Copyright 2011 The Royal Society of Chemistry.

modulation of FRET efficiencies. Upon UV irradiation at pH 8.5, DMNA moieties within microgels undergo photolysis reactions and form sodium carboxylate residues on the microgel scaffold, and this results in elevated VPT temperature. Thus, UV irradiation of microgel dispersions at the intermediate temperature range (between the VPT temperature of original microgels and that of UV-irradiated microgels) can directly lead to the re-swelling of initially collapsed microgels. The incorporation of FRET pairs (NBDAE and RhBEA dyes) allows for the *in situ* monitoring of thermo and UV irradiation-induced VPT processes. This work represents the first report of polymeric NPs-based FRET systems with thermo- and photo-tunable FRET efficiency.

On the basis of a similar strategy, Yin *et al.*[132] and Wang *et al.*[133] replaced photocleavable DMNA moieties with K^+-recognizing 4-acrylamidobenzo-18-crown-6 residues (B18C6Am) and glucose-recognizing *N*-acryloyl-3-aminophenylboronic acid (APBA), respectively, to construct microgel-based FRET systems. The FRET efficiency of fluorescent microgels can be tuned by the addition of K^+ and glucose, respectively, by taking advantage of supramolecular recognition of K^+-crown ether and glucose–phenylboronic acid pairs. These processes correspondingly induce changes in the hydrophilicity/hydrophobicity balance, affecting VPT temperatures of thermoresponsive microgels. The spatial distance between fluorescent donors and acceptors (NBDAE and RhBEA) within microgels can then be tuned *via* thermo-induced collapse/swelling of thermo-responsive microgels or the addition of K^+ ions and glucose at intermediate temperature ranges.

Hu *et al.*[134] recently found that upon addition of fluoride ions (F^-), the green fluorescence emission of NBDAE moieties can be dramatically quenched. By taking advantage of the F^--responsive NBDAE emission, they designed a novel type of ratiometric fluorescent polymeric probes for F^- ions based on self-assembled micellar NPs of the P(MMA-*co*-NBDAE)-*b*-PF-*b*-P-(MMA-*co*-NBDAE) coil–rod–coil triblock copolymer, where MMA and PF are methyl methacrylate and polyfluorene, respectively (Fig. 13).[135] Blue-emitting conjugated PF block and green-emitting NBDAE moieties within the PMMA block serve as FRET donors and switchable acceptors, respectively. In acetone, the triblock copolymer spontaneously self-assembles into micelles possessing PF cores and NBDAE-labeled PMMA coronas. Upon addition of F^- ions, the quenching of NBDAE emission bands turns off the FRET processes between micellar cores and coronas, leading to ~8.75-fold decrease in the emission intensity ratio, I_{515}/I_{417}. As compared to that of molecularly dissolved chains in THF, self-assembled micelles of coil–rod–coil triblock copolymers serve as better ratiometric fluorescent F^- ion sensors possessing visual detection capability.

Very recently, Peng and Wolfbeis *et al.*[136] designed biocompatible fluorescent polyurethane nanogels for intracellular pH sensing by loading into nanogels with a pH indicator dye, bromothymol blue (BTB), and two additional fluorophores that undergo efficient FRET processes within nanogels. Coumarin 6 (C6) and NR were chosen as fluorescent donor and acceptor, respectively, to give a dual fluorescent signal which can be quantified in a ratiometric manner. Upon excitation of C6 at 440 nm, green fluorescence emission at 520 nm is observed, accompanied with partial FRET to NR residues emitting at around 620 nm. BTB is a pH-sensitive dye which is yellow at pH < 6 with an absorption maximum at around 535 nm, which overlaps with the green C6 emission, and turns blue at pH > 8 with an absorption maximum at 628 nm, which overlaps with the red emission of the NR acceptor. Thus, the energy transfer from C6 or NR to BTB under low and high pH conditions, respectively, resulted in large changes

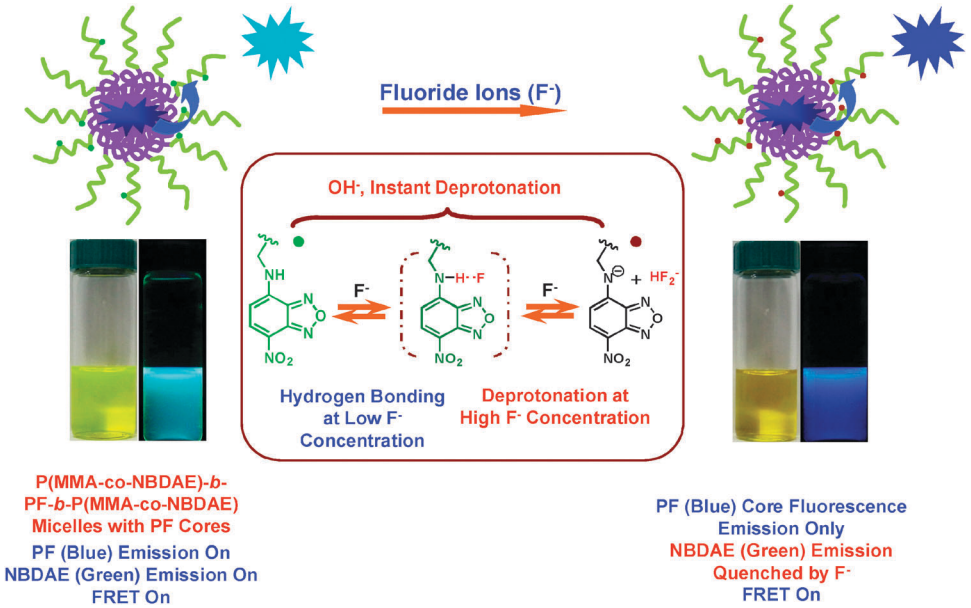

Fig. 13 Schematic illustration of P(MMA-*co*-NBDAE)-*b*-PF-*b*-P(MMA-*co*-NBDAE) triblock copolymer micelles consisting of blue-emitting polyfluorene (PF) cores and green-emitting P(MMA-*co*-NBDAE) coronas, which can serve as ratiometric fluorescent probes for fluoride ions. Reproduced with permission from ref. 135. Copyright 2011 American Chemical Society.

in relative fluorescence intensity ratios of C6 and NR emissions due to pH-dependent changes of BTB absorption. Considering its facile design, this approach is likely to exhibit a broad scope for intracellular biosensing.

4.3. The combination of off–on switching of FRET processes and FRET efficiency modulation

The design of fluorescent polymeric assemblies and NPs combining characteristics of off–on switching of FRET processes and further tuning the FRET efficiency by taking advantage of stimuli-sensitive fluorophores and the responsive polymer matrix, respectively, actually represent another intriguing research direction. These can endow fluorescent polymeric assemblies and NPs with multi-functionality and enhanced designing flexibility and structural adaptability.

In a notable example, Wu *et al.*[137] reported the fabrication of photoswitchable and thermo-tunable multicolor fluorescent hybrid organic/inorganic hybrid PNIPAM brushes. Within the fluorescent hybrid NPs, the FRET process between NBDAE (FRET donor) and SP moieties (FRET acceptor) can be reversibly switched on/off *via* UV/visible light irradiation, and after the FRET process was switched on, the FRET efficiency can be further modulated by temperature variation. They synthesized silica/PNIPAM hybrid NPs coated with PNIPAM brushes of two layers, with the inner and outer layers covalently labeled with NBDAE dyes and SP moieties, respectively, *via* consecutive ATRP copolymerization of NIPAM with specific fluorescent dyes-based monomers from the surface of silica NPs. Under visible light irradiation, the hybrid NPs exhibit green emission from NBDAE dyes, whereas the SP-labeled outer PNIPAM layer is non-emissive. Heating the aqueous dispersion of hybrid NPs leads to enhanced fluorescence signals of NBDAE moieties due to the more hydrophobic microenvironments induced by the collapse of PNIPAM brushes. UV-induced ring-opening reaction of SP moieties switched on the FRET process between NBDAE in the inner layer and ring-opened MC form of SP moieties in the outer layer. Moreover, upon heating, the FRET efficiency can be further dramatically enhanced due to decreased spatial distances between fluorescent donors and acceptors, resulting from the collapse of PNIPAM brushes at elevated temperatures. Based on thermo-responsive diblock copolymer micelles, we also constructed a series of dual fluorescent multifunctional chemosensors for temperature and other analytes such as Hg^{2+} and pH (Fig. 14).[56,138]

Recently, Yin *et al.*[139] designed thermo-responsive PNIPAM microgel-based Cu^{2+} sensors with thermo-tunable sensitivity. Within microgels, dansyl-containing fluorescence reporter (DAEAM) and metal-chelating moiety, *N*-(2-(2-oxo-2-(pyridine-2-yl-methylamino)ethylamino) ethyl)acrylamide (PyAM) ligand were covalently labeled. The binding of Cu^{2+} ions by PyAM turns on the FRET process between DAEAM and Cu^{2+}–PyAM complex, leading to the fluorescence quenching of DAEAM. The FRET efficiency (quenching efficiency) largely depends on the relative distance between the Cu^{2+} complex and DAEAM. Upon heating above the VPT temperature, the dramatically decreased average distance between neighboring PyAM and DAEAM moieties leads to enhanced FRET efficiency (quenching efficiency). Within collapsed PNIPAM microgels at elevated temperatures, the more effective binding with Cu^{2+} and close proximity between DAEAM moieties and PyAM/Cu^{2+} complex both contributed to the enhanced detection sensitivity.

It is worth noting that in the above described examples, there is just one single FRET process which can be switched on and off by external stimuli, *i.e.*, the stimuli-switching of fluorescence emission within polymeric assemblies and NPs is conducted over two states. Very recently, we constructed the first system of reversible three-state switching of multicolor thermo-responsive polymeric micelles based on amphiphilic diblock co-polymers, P(St-*co*-NBDAE-*co*-SPMA)-*b*-P(NIPAM-*co*-RhBAM).

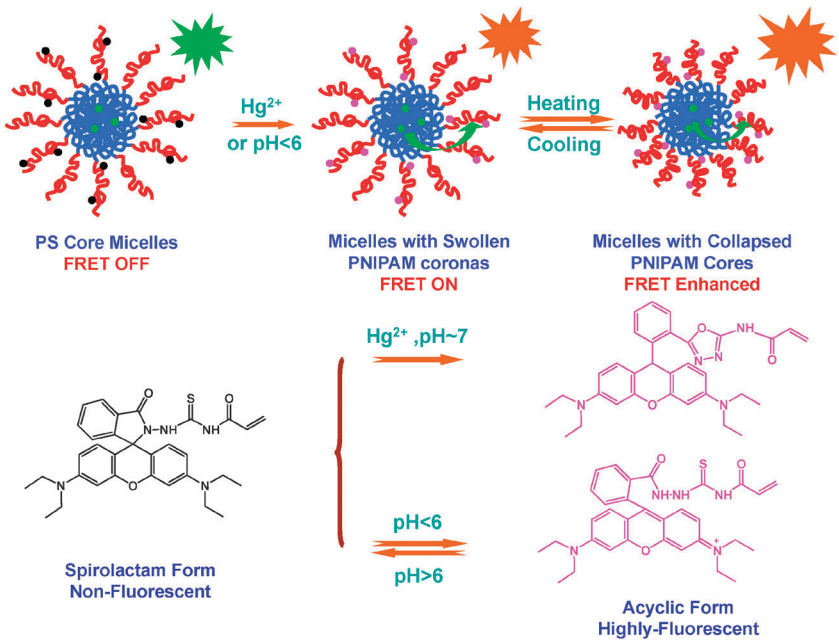

Fig. 14 Schematic illustration of the construction of P(St-*co*-NBDAE)-*b*-P(NIPAM-*co*-RhBHA) amphiphilic thermo-responsive diblock copolymer micelles-based multifunctional ratiometric fluorescent chemosensors for Hg^{2+}, pH, and temperature. Reproduced with permission from ref. 56. Copyright 2011 American Chemical Society.

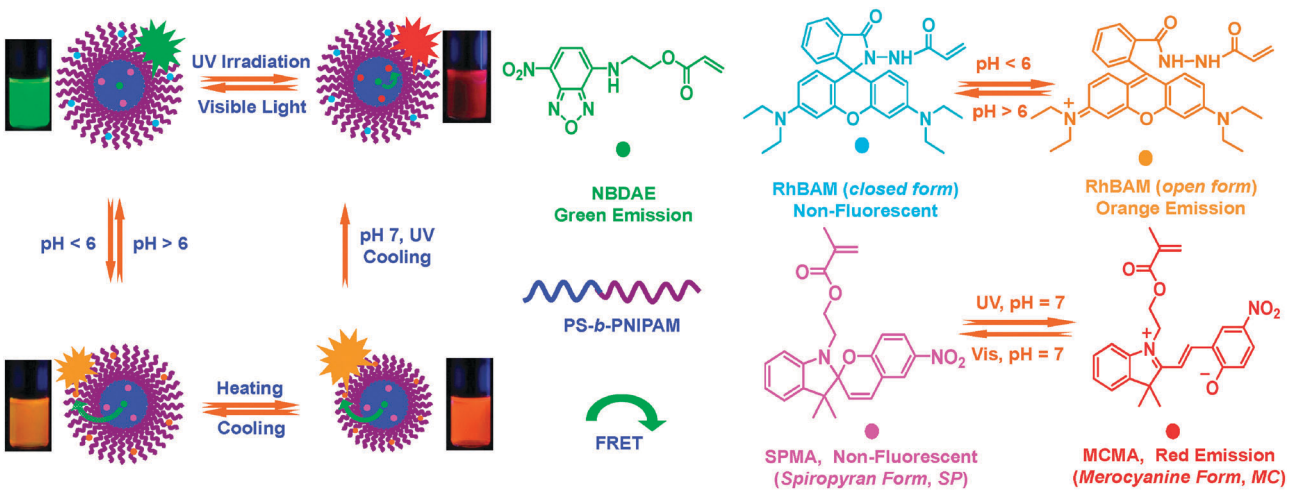

Fig. 15 Schematic illustration of the construction of polymeric micelles-based reversible three-state switchable multicolor luminescent system fabricated from amphiphilic and thermo-responsive diblock copolymer, P(St-*co*-NBDAE-*co*-SPMA)-*b*-P(NIPAM-*co*-RhBAM), bearing NBDAE and photo-switchable SPMA fluorophores in the hydrophobic PS block and pH-switchable RhBAM dyes in the thermo-responsive PNIPAM block. Also shown are macroscopic images recorded under UV light. Reproduced with permission from ref. 140. Copyright 2010 Wiley-VCH.

The FRET donor (NBDAE) and two types of acceptors, pH-switchable RhBAM and photoswitchable SPMA, were all covalently attached to diblock copolymer chains (Fig. 15).[140] On/off fluorescence switching of the latter two types of acceptor dyes can be controlled by pH changes and light, respectively. RhBAM moieties are non-fluorescent at pH $>$ 6 and highly emissive at pH $<$ 6. Thus, this novel type of dye combination facilely leads to the construction of three-state switchable multi-color luminescent systems: (a) NBDAE emission at pH 7 under visible light; (b) NBDAE/RhBAM (open form) FRET system below pH 6 under visible light; (c) NBDAE/MCMA FRET system at pH 7 upon UV irradiation. Moreover, the efficiency of the FRET process between NBDAE and ring-opened RhBAM below pH 6 can be facilely tuned by temperature variations by exploiting the thermo-induced collapse of PNIPAM coronas of diblock copolymer micelles, which results in the closer proximity between FRET donors and acceptors.

5. Conclusions

Fluorescent chemosensors and biosensors render *in vitro* and *in vivo* biological assays and *in situ* process monitoring much more facile with exquisite sensitivity and selectivity. Nanosized fluorescent polymeric assemblies and NPs have now become a fascinating new tool in this field by taking advantage of their photostability, stimuli-responsiveness, aqueous dispersibility,

good biocompatibility, versatility in design and structural control, and the ability of further functionalization. Moreover, the chemical composition and morphology of these polymeric assemblies and NPs can be easily modulated through synthetic approaches, leading to the precise spatial organization of multiple fluorophores. In addition, polymeric assemblies and NPs can be physically embedded or covalently labeled with two or more emitting fluorophores. By employing nanosized polymeric assemblies or NPs as the scaffolds, the once challenging task of building sophisticated FRET systems has been rendered much easier. The strategies employed in designing fluorescent polymeric assemblies and NPs with external stimuli-tunable emission characteristics cover three main types, namely, lighting up fluorescence, tuning fluorescence emission, and modulating FRET processes.

From these selected examples, we can see a fast-growing trend in the exploitation of polymeric assemblies and NPs as fluorescent scaffolds, and more and more research groups have become involved in this field. However, the challenge still remains. In particular, the relevant specific biomedical applications (*e.g.* biosensing, biolabeling, and bioimaging) are still quite limited. Fluorescent assemblies and NPs exhibiting selective emission turn-on or the switching on and turn-off of the FRET process under specific biological milieu (*e.g.* intracellular, tumor tissue or disease site, cell surface antigens and receptors, specific enzymes) are highly desirable.

Future works need to be conducted concerning further improvement of the stability, biocompatibility, and biodegradability of stimuli-responsive fluorescent polymeric assemblies and NPs. Novel and more biocompatible covalent or non-covalent stabilization chemistries (*e.g.* shell or core cross-linking strategies) need to be explored to achieve long-term structural stability._ENREF_135 Controlled functionalization of fluorescent polymeric assemblies and NPs with tumor cell, disease tissue, and specific intracellular organelle-targeting moieties will further improve their potential *in vivo* applications. In addition, the integration of fluorescence imaging and sensing capabilities with other sophisticated clinical diagnosis techniques such as magnetic resonance (MR) imaging, positron emission tomography (PET), and X-ray computed tomography (CT) will allow for the construction of multimodal and multifunctional polymeric assemblies and NPs. Moreover, the exploitation of fluorescent polymeric assemblies and NPs as controlled release chemotherapeutic drug, gene, and protein nanocarriers will render possible the next generation personalized theranostic system, which will also allow for the *in situ* monitoring of drug biodistribution, pharmacokinetics, and intracellular metabolism pathways. Finally, considering that UV irradiation is in general harmful to living organisms and organic fluorophores that are typically subjected to photobleaching, fluorescent polymeric assemblies and NPs bearing NIR-excitable fluorophores or two-photon absorbing dyes or embedded with upconversion inorganic nanoparticles are in high demand, which represents an emerging research direction. Overall, the selected recent works discussed in this feature article are supposed to further stimulate fresh perspectives and new ideas, aiming at exploring and developing more sophisticated responsive polymeric assemblies and NP-based functional systems.

Acknowledgements

The financial support from National Natural Scientific Foundation of China (NNSFC) Project (51033005, 20874092, and 91027026) and Fundamental Research Funds for the Central Universities is gratefully acknowledged.

References

1 A. P. Demchenko, *Introduction to Fluorescence Sensing*, Springer, Berlin/Heidelberg, 2008.
2 R. Martínez-Máñez and F. Sancenón, *Chem. Rev.*, 2003, **103**, 4419–4476.
3 K. Rurack and U. Resch-Genger, *Chem. Soc. Rev.*, 2002, **31**, 116–127.
4 W. S. Han, H. Y. Lee, S. H. Jung, S. J. Lee and J. H. Jung, *Chem. Soc. Rev.*, 2009, **38**, 1904–1915.
5 F. Mancin, E. Rampazzo, P. Tecilla and U. Tonellato, *Chem.–Eur. J.*, 2006, **12**, 1844–1854.
6 L. Prodi, *New J. Chem.*, 2005, **29**, 20–31.
7 L. Prodi, F. Bolletta, M. Montalti and N. Zaccheroni, *Coord. Chem. Rev.*, 2000, **205**, 59–83.
8 A. P. de Silva, H. Q. N. Gunaratne, T. Gunnlaugsson, A. J. M. Huxley, C. P. McCoy, J. T. Rademacher and T. E. Rice, *Chem. Rev.*, 1997, **97**, 1515–1566.
9 K. E. Sapsford, L. Berti and I. L. Medintz, *Angew. Chem., Int. Ed.*, 2006, **45**, 4562–4588.
10 S. F. Martin, M. H. Tatham, R. T. Hay and I. D. W. Samuel, *Protein Sci.*, 2008, **17**, 777–784.
11 S. Jiwpanich, J. H. Ryu, S. Bickerton and S. Thayumanavan, *J. Am. Chem. Soc.*, 2010, **132**, 10683–10685.
12 S. W. A. Reulen and M. Merkx, *Bioconjugate Chem.*, 2010, **21**, 860–866.
13 C. Pietsch, U. S. Schubert and R. Hoogenboom, *Chem. Commun.*, 2011, **47**, 8750–8765.
14 J. M. Hu and S. Y. Liu, *Macromolecules*, 2010, **43**, 8315–8330.
15 H. N. Kim, Z. Guo, W. Zhu, J. Yoon and H. Tian, *Chem. Soc. Rev.*, 2011, **40**, 79–93.
16 L. Bau, P. Tecilla and F. Mancin, *Nanoscale*, 2011, **3**, 121–133.
17 Y. Shiraishi, R. Miyamoto, X. Zhang and T. Hirai, *Org. Lett.*, 2007, **9**, 3921–3924.
18 Y. Shiraishi, T. Inoue and T. Hirai, *Langmuir*, 2010, **26**, 17505–17512.
19 Y. Shiraishi, R. Miyarnoto and T. Hirai, *Langmuir*, 2008, **24**, 4273–4279.
20 D. P. Wang, R. Miyamoto, Y. Shiraishi and T. Hirai, *Langmuir*, 2009, **25**, 13176–13182.
21 Q. Yan, J. Y. Yuan, W. Z. Yuan, M. Zhou, Y. W. Yin and C. Y. Pan, *Chem. Commun.*, 2008, 6188–6190.
22 V. V. Rostovtsev, L. G. Green, V. V. Fokin and K. B. Sharpless, *Angew. Chem., Int. Ed.*, 2002, **41**, 2596–2599.
23 K. B. Sharpless, *Angew. Chem., Int. Ed.*, 2002, **41**, 2024–2032.
24 B. S. Sumerlin and A. P. Vogt, *Macromolecules*, 2009, **43**, 1–13.
25 M. F. Cunningham, *Prog. Polym. Sci.*, 2002, **27**, 1039–1067.
26 W. A. Braunecker and K. Matyjaszewski, *Prog. Polym. Sci.*, 2007, **32**, 93–146.
27 C. J. Hawker, A. W. Bosman and E. Harth, *Chem. Rev.*, 2001, **101**, 3661–3688.
28 V. Coessens, T. Pintauer and K. Matyjaszewski, *Prog. Polym. Sci.*, 2001, **26**, 337–377.
29 M. Ouchi, T. Terashima and M. Sawamoto, *Chem. Rev.*, 2009, **109**, 4963–5050.
30 J. Chiefari, Y. K. Chong, F. Ercole, J. Krstina, J. Jeffery, T. P. T. Le, R. T. A. Mayadunne, G. F. Meijs, C. L. Moad, G. Moad, E. Rizzardo and S. H. Thang, *Macromolecules*, 1998, **31**, 5559–5562.
31 A. E. Smith, X. Xu and C. L. McCormick, *Prog. Polym. Sci.*, 2010, **35**, 45–93.
32 A. B. Lowe and C. L. McCormick, *Prog. Polym. Sci.*, 2007, **32**, 283–351.
33 M. Beija, M.-T. Charreyre and J. M. G. Martinho, *Prog. Polym. Sci.*, 2011, **36**, 568–602.
34 I. Lee, Y. Yoo, Z. Cheng and H. K. Jeong, *Adv. Funct. Mater.*, 2008, **18**, 4014–4021.

35 S. H. Bae, S. Il Yoo, W. K. Bae, S. Lee, J. K. Lee and B. H. Sohn, *Chem. Mater.*, 2008, **20**, 4185–4187.
36 J. Peng, M. Chen, F. Qiu, Y. Yang, B. H. Sohn and D. H. Kim, *Appl. Phys. Lett.*, 2008, **93**, 183303.
37 S. I. Yoo, S. H. Bae, K. S. Kim and B. H. Sohn, *Soft Matter*, 2009, **5**, 2990–2996.
38 S. I. Yoo, J.-H. Lee, B.-H. Sohn, I. Eom, T. Joo, S. J. An and G.-C. Yi, *Adv. Funct. Mater.*, 2008, **18**, 2984–2989.
39 H. G. Schild, *Prog. Polym. Sci.*, 1992, **17**, 163–249.
40 R. Pelton, *Adv. Colloid Interface Sci.*, 2000, **85**, 1–33.
41 S. Dai, P. Ravi and K. C. Tam, *Soft Matter*, 2009, **5**, 2513–2533.
42 S. Dai, P. Ravi and K. C. Tam, *Soft Matter*, 2008, **4**, 435–449.
43 C. D. H. Alarcon, S. Pennadam and C. Alexander, *Chem. Soc. Rev.*, 2005, **34**, 276–285.
44 D. Roy, J. N. Cambre and B. S. Sumerlin, *Prog. Polym. Sci.*, 2010, **35**, 278–301.
45 C. Weber, R. Hoogenboom and U. S. Schubert, *Prog. Polym. Sci.*, 2012, DOI: 10.1016/j.progpolymsci.2011.10.002.
46 J. V. M. Weaver, S. P. Armes and S. Y. Liu, *Macromolecules*, 2003, **36**, 9994–9998.
47 D. Wang, J. Yin, Z. Y. Zhu, Z. S. Ge, H. W. Liu, S. P. Armes and S. Y. Liu, *Macromolecules*, 2006, **39**, 7378–7385.
48 J. Xu, J. Ye and S. Y. Liu, *Macromolecules*, 2007, **40**, 9103–9110.
49 Y. M. Zhou, K. Q. Jiang, Q. L. Song and S. Y. Liu, *Langmuir*, 2007, **23**, 13076–13084.
50 H. X. Xu, J. Xu, Z. Y. Zhu, H. W. Liu and S. Y. Liu, *Macromolecules*, 2006, **39**, 8451–8455.
51 Z. S. Ge, J. M. Hu, F. H. Huang and S. Y. Liu, *Angew. Chem., Int. Ed.*, 2009, **48**, 1798–1802.
52 Y. K. Yang, K. J. Yook and J. Tae, *J. Am. Chem. Soc.*, 2005, **127**, 16760–16761.
53 X. L. Zhang, Y. Xiao and X. H. Qian, *Angew. Chem., Int. Ed.*, 2008, **47**, 8025–8029.
54 Y. Xiang and A. J. Tong, *Org. Lett.*, 2006, **8**, 1549–1552.
55 J. M. Hu, C. H. Li and S. Y. Liu, *Langmuir*, 2010, **26**, 724–729.
56 J. M. Hu, L. Dai and S. Y. Liu, *Macromolecules*, 2011, **44**, 4699–4710.
57 X. J. Wan and S. Y. Liu, *J. Mater. Chem.*, 2011, **21**, 10321–10329.
58 T. Liu and S. Y. Liu, *Anal. Chem.*, 2011, **83**, 2775–2785.
59 Y. Y. Jiang, X. L. Hu, J. M. Hu, H. Liu, H. Zhong and S. Y. Liu, *Macromolecules*, 2011, **44**, 8780–8790.
60 R. Guglielmetti, *Photochromism: Molecules and Systems*, Elsevier, Amsterdam, revised edn, 2003.
61 M. Irie, *Chem. Rev.*, 2000, **100**, 1685–1716.
62 G. Berkovic, V. Krongauz and V. Weiss, *Chem. Rev.*, 2000, **100**, 1741–1754.
63 M. Irie, T. Fukaminato, T. Sasaki, N. Tamai and T. Kawai, *Nature*, 2002, **420**, 759–760.
64 M. Q. Zhu, L. Y. Zhu, J. J. Han, W. W. Wu, J. K. Hurst and A. D. Q. Li, *J. Am. Chem. Soc.*, 2006, **128**, 4303–4309.
65 M. Q. Zhu, G. F. Zhang, C. Li, M. P. Aldred, E. Chang, R. A. Drezek and A. D. Q. Li, *J. Am. Chem. Soc.*, 2011, **133**, 365–372.
66 V. I. Minkin, *Chem. Rev.*, 2004, **104**, 2751–2776.
67 J. D. Luo, Z. L. Xie, J. W. Y. Lam, L. Cheng, H. Y. Chen, C. F. Qiu, H. S. Kwok, X. W. Zhan, Y. Q. Liu, D. B. Zhu and B. Z. Tang, *Chem. Commun.*, 2001, 1740–1741.
68 B.-K. An, S.-K. Kwon, S.-D. Jung and S. Y. Park, *J. Am. Chem. Soc.*, 2002, **124**, 14410–14415.
69 Y. N. Hong, J. W. Y. Lam and B. Z. Tang, *Chem. Commun.*, 2009, 4332–4353.
70 Y. N. Hong, J. W. Y. Lam and B. Z. Tang, *Chem. Soc. Rev.*, 2011, **40**, 5361–5388.
71 C. Le Droumaguet, C. Wang and Q. Wang, *Chem. Soc. Rev.*, 2010, **39**, 1233–1239.
72 K. Sivakumar, F. Xie, B. M. Cash, S. Long, H. N. Barnhill and Q. Wang, *Org. Lett.*, 2004, **6**, 4603–4606.
73 Z. Zhou and C. J. Fahrni, *J. Am. Chem. Soc.*, 2004, **126**, 8862–8863.
74 R. K. O'Reilly, M. J. Joralemon, C. J. Hawker and K. L. Wooley, *Chem.–Eur. J.*, 2006, **12**, 6776–6786.
75 D. R. Breed, R. Thibault, F. Xie, Q. Wang, C. J. Hawker and D. J. Pine, *Langmuir*, 2009, **25**, 4370–4376.
76 C. E. Evans and P. A. Lovell, *Chem. Commun.*, 2009, 2305–2307.
77 A. J. Dirks, J. J. L. M. Cornelissen and R. J. M. Nolte, *Bioconjugate Chem.*, 2009, **20**, 1129–1138.
78 A. D. Ievins, X. F. Wang, A. O. Moughton, J. Skey and R. K. O'Reilly, *Macromolecules*, 2008, **41**, 2998–3006.
79 M. Sawa, T. L. Hsu, T. Itoh, M. Sugiyama, S. R. Hanson, P. K. Vogt and C. H. Wong, *Proc. Natl. Acad. Sci. U. S. A.*, 2006, **103**, 12371–12376.
80 S. Lee, J. H. Ryu, K. Park, A. Lee, S. Y. Lee, I. C. Youn, C. H. Ahn, S. M. Yoon, S. J. Myung, D. H. Moon, X. Chen, K. Choi, I. C. Kwon and K. Kim, *Nano Lett.*, 2009, **9**, 4412–4416.
81 M. Oishi, A. Tamura, T. Nakamura and Y. Nagasaki, *Adv. Funct. Mater.*, 2009, **19**, 827–834.
82 M.-P. Chien, M. P. Thompson and N. C. Gianneschi, *Chem. Commun.*, 2011, **47**, 167–169.
83 L. Tang, J. K. Jin, A. J. Qin, W. Z. Yuan, Y. Mao, J. Mei, J. Z. Sun and B. Z. Tang, *Chem. Commun.*, 2009, 4974–4976.
84 Y. Liu, C. M. Deng, L. Tang, A. J. Qin, R. R. Hu, J. Z. Sun and B. Z. Tang, *J. Am. Chem. Soc.*, 2010, **133**, 660–663.
85 L. Tang, J. K. Jin, S. Zhang, Y. Mao, J. Z. Sun, W. Z. Yuan, H. Zhao, H. P. Xu, A. J. Qin and B. Z. Tang, *Sci. China, Ser. B: Chem.*, 2009, **52**, 755–759.
86 C. H. Li, J. M. Hu, T. Liu and S. Y. Liu, *Macromolecules*, 2011, **44**, 429–431.
87 C. H. Li, T. Wu, C. Y. Hong, G. Q. Zhang and S. Y. Liu, *Angew. Chem., Int. Ed.*, 2012, **51**, 455–459.
88 E. Y. Bryleva, N. A. Vodolazkaya, N. O. Mchedlov-Petrossyan, L. V. Samokhina, N. A. Maveevskaya and A. V. Tolmachev, *J. Colloid Interface Sci.*, 2007, **316**, 712–722.
89 H. Sun, A. M. Scharff-Poulsen, H. Gu and K. Almdal, *Chem. Mater.*, 2006, **18**, 3381–3384.
90 E. Allard and C. Larpent, *J. Polym. Sci., Part A: Polym. Chem.*, 2008, **46**, 6206–6213.
91 S. Hornig, C. Biskup, A. Grafe, J. Wotschadlo, T. Liebert, G. J. Mohr and T. Heinze, *Soft Matter*, 2008, **4**, 1169–1172.
92 J. W. Tian, H. C. Chen, L. H. Zhuo, Y. X. Xie, N. Li and B. Tang, *Chem.–Eur. J.*, 2011, **17**, 6626–6634.
93 R. Huang, D. Y. Chen and M. Jiang, *J. Mater. Chem.*, 2010, **20**, 9988–9994.
94 S. Uchiyama, Y. Matsumura, A. P. de Silva and K. Iwai, *Anal. Chem.*, 2003, **75**, 5926–5935.
95 S. Uchiyama, N. Kawai, A. P. de Silva and K. Iwai, *J. Am. Chem. Soc.*, 2004, **126**, 3032–3033.
96 S. Uchiyama, Y. Matsumura, A. P. de Silva and K. Iwai, *Anal. Chem.*, 2004, **76**, 1793–1798.
97 K. Iwai, Y. Matsumura, S. Uchiyama and A. P. de Silva, *J. Mater. Chem.*, 2005, **15**, 2796–2800.
98 S. Uchiyama and Y. Makino, *Chem. Commun.*, 2009, 2646–2648.
99 C. Gota, S. Uchiyama and T. Ohwada, *Analyst*, 2007, **132**, 121–126.
100 C. Gota, S. Uchiyama, T. Yoshihara, S. Tobita and T. Ohwada, *J. Phys. Chem. B*, 2008, **112**, 2829–2836.
101 C. Gota, K. Okabe, T. Funatsu, Y. Harada and S. Uchiyama, *J. Am. Chem. Soc.*, 2009, **131**, 2766–2767.
102 F. Li, A. H. Westphal, A. T. M. Marcelis, E. J. R. Sudholter, M. A. Cohen Stuart and F. A. M. Leermakers, *Soft Matter*, 2011, **7**, 11211–11215.
103 C. Pietsch, R. Hoogenboom and U. S. Schubert, *Polym. Chem.*, 2010, **1**, 1005–1008.
104 C. Pietsch, A. Vollrath, R. Hoogenboom and U. S. Schubert, *Sensors*, 2010, **10**, 7979–7990.
105 C. Y. Chen and C. T. Chen, *Chem. Commun.*, 2011, **47**, 994–996.
106 A. S. Klymchenko, G. Duportail, A. P. Demchenko and Y. Mely, *Biophys. J.*, 2004, **86**, 2929–2941.
107 A. P. Demchenko, A. S. Klymchenko, V. G. Pivovarenko, S. Ercelen, G. Duportail and Y. Mely, *J. Fluoresc.*, 2003, **13**, 291–295.
108 P.-T. Chou, W.-S. Yu, Y.-M. Cheng, S.-C. Pu, Y.-C. Yu, Y.-C. Lin, C.-H. Huang and C.-T. Chen, *J. Phys. Chem. A*, 2004, **108**, 6487–6498.
109 P.-T. Chou, C.-H. Huang, S.-C. Pu, Y.-M. Cheng, Y.-H. Liu, Y. Wang and C.-T. Chen, *J. Phys. Chem. A*, 2004, **108**, 6452–6454.
110 K. Aslan, J. Zhang, J. R. Lakowicz and C. D. Geddes, *J. Fluoresc.*, 2004, **14**, 391–400.
111 W. T. Wu, N. Mitra, E. C. Y. Yan and S. Q. Zhou, *ACS Nano*, 2010, **4**, 4831–4839.
112 G. Vancoillie, S. Pelz, E. Holder and R. Hoogenboom, *Polym. Chem.*, 2012, DOI: 10.1039/C1PY00380A.

113 K. J. Zhou, Y. G. Wang, X. N. Huang, K. Luby-Phelps, B. D. Sumer and J. M. Gao, *Angew. Chem., Int. Ed.*, 2011, **50**, 6109–6114.
114 W. T. Wu, T. Zhou, M. Aiello and S. Q. Zhou, *Chem. Mater.*, 2009, **21**, 4905–4913.
115 Y. Y. Li, H. Cheng, J. L. Zhu, L. Yuan, Y. Dai, S. X. Cheng, X. Z. Zhang and R. X. Zhuo, *Adv. Mater.*, 2009, **21**, 2402–2406.
116 C. H. Li and S. Y. Liu, *J. Mater. Chem.*, 2010, **20**, 10716–10723.
117 T. Liu, J. M. Hu, J. Yin, Y. F. Zhang, C. H. Li and S. Y. Liu, *Chem. Mater.*, 2009, **21**, 3439–3446.
118 X. J. Wan, T. Liu and S. Y. Liu, *Langmuir*, 2011, **27**, 4082–4090.
119 L. Y. Zhu, W. W. Wu, M. Q. Zhu, J. J. Han, J. K. Hurst and A. D. Q. Li, *J. Am. Chem. Soc.*, 2007, **129**, 3524–3526.
120 J. Chen, F. Zeng and S. Z. Wu, *ChemPhysChem*, 2010, **11**, 1036–1043.
121 J. Chen, F. Zeng, S. Z. Wu, Q. M. Chen and Z. Tong, *Chem.–Eur. J.*, 2008, **14**, 4851–4860.
122 J. Chen, F. Zeng, S. Z. Wu, J. Q. Zhao, Q. M. Chen and Z. Tong, *Chem. Commun.*, 2008, 5580–5582.
123 J. A. Chen, P. S. Zhang, G. Fang, P. G. Yi, X. Y. Yu, X. F. Li, F. Zeng and S. Z. Wu, *J. Phys. Chem. B*, 2011, **115**, 3354–3362.
124 I. Yildiz, S. Impellizzeri, E. Deniz, B. McCaughan, J. F. Callan and F. M. Raymo, *J. Am. Chem. Soc.*, 2011, **133**, 871–879.
125 B. L. Ma, S. Z. Wu, F. Zeng, Y. L. Luo, J. Q. Zhao and Z. Tong, *Nanotechnology*, 2010, **21**, 195501–195509.
126 J. Chen, F. Zeng, S. Z. Wu, J. H. Su, J. Q. Zhao and Z. Tong, *Nanotechnology*, 2009, **20**, 365502–365508.
127 M. Frigoli, K. Ouadahi and C. Larpent, *Chem.–Eur. J.*, 2009, **15**, 8319–8330.
128 I. L. Medintz, H. T. Uyeda, E. R. Goldman and H. Mattoussi, *Nat. Mater.*, 2005, **4**, 435–446.
129 Y. J. Gong, M. Y. Gao, D. Y. Wang and H. Mohwald, *Chem. Mater.*, 2005, **17**, 2648–2653.
130 L. Ionov and S. Diez, *J. Am. Chem. Soc.*, 2009, **131**, 13315–13319.
131 J. Yin, H. B. Hu, Y. H. Wu and S. Y. Liu, *Polym. Chem.*, 2011, **2**, 363–371.
132 J. Yin, C. H. Li, D. Wang and S. Y. Liu, *J. Phys. Chem. B*, 2010, **114**, 12213–12220.
133 D. Wang, T. Liu, J. Yin and S. Y. Liu, *Macromolecules*, 2011, **44**, 2282–2290.
134 J. M. Hu, C. H. Li, Y. Cui and S. Y. Liu, *Macromol. Rapid Commun.*, 2011, **32**, 610–615.
135 J. M. Hu, G. Y. Zhang, Y. H. Geng and S. Y. Liu, *Macromolecules*, 2011, **44**, 8207–8214.
136 H. S. Peng, J. A. Stolwijk, L. N. Sun, J. Wegener and O. S. Wolfbeis, *Angew. Chem., Int. Ed.*, 2010, **49**, 4246–4249.
137 T. Wu, G. Zou, J. M. Hu and S. Y. Liu, *Chem. Mater.*, 2009, **21**, 3788–3798.
138 J. M. Hu, X. Z. Zhang, D. Wang, X. L. Hu, T. Liu, G. Y. Zhang and S. Y. Liu, *J. Mater. Chem.*, 2011, **21**, 19030–19038.
139 J. Yin, X. F. Guan, D. Wang and S. Y. Liu, *Langmuir*, 2009, **25**, 11367–11374.
140 C. H. Li, Y. X. Zhang, J. M. Hu, J. J. Cheng and S. Y. Liu, *Angew. Chem., Int. Ed.*, 2010, **49**, 5120–5124.

